Response to Reviewer 1

We greatly appreciate the time and effort that reviewer 1 spent in reviewing our manuscript. The comments are really thoughtful and helpful to improve the quality of our paper. Reviewer 1 has provided both main comments and other specific comments. Below we make a point-by-point response to these comments. According to editor's requirement, the response to the referee 1 is structured in the following sequence: (1) comments from the referee in black color, (2) our response in blue color, and (3) our changes in the revised manuscript in red color.

Zhang et al. presented a chamber study that examined the effect of RH on SOA mass yields and composition. This paper is potentially useful to the SOA community. However, there are portions of the manuscripts that need to be addressed before the manuscript can be considered for publication.

1. Page 4 line 3: Clarify how H2O2 and m-xylene were introduced into the chamber. Via an injection into a glass bulb using a syringe? Using a bubbler? How did the authors determine when the chamber contained 20 ppm of H2O2? Was the concentration of gas-phase H2O2 in the chamber measured in real-time? If yes, what instrument was used?

H_2O_2 and *m*-xylene were introduced into the reactor along with the zero air flow via an injection into a three-way tube using a syringe. The concentration of gas-phase H_2O_2 in the reactor was not measured but calculated. To obtain a certain concentration of H_2O_2, the density and mass concentration of injected H_2O_2 solution, and the volume of the reactor were used to calculate the volume of H_2O_2 solution that needed to be injected.

2. Page 4 line 5: Explain the rationale behind not using any seed aerosols in this study. Seed aerosols are typically used in chamber studies to promote the condensation of SOA-forming vapors onto seed aerosol instead of the chamber walls. The mass yields reported by the authors are likely under-estimated since most of the vapors are likely lost the chamber walls in these experiments (See examples provided in Zhang et al., PNAS 2014, Nah et al., ACP 2016, 2017). Vapor wall loss is also going to affect the types of products formed in these SOA experiments since highly oxygenated and least volatile compounds are lost to the chamber walls are faster rates (See Zhang et al., ACP 2015). The authors should comment on how vapor wall loss affects their results. Can they also provide an estimation on how much their SOA mass yields are underestimated by?

Nah, T., McVay, R. C., Zhang, X., Boyd, C. M., Seinfeld, J. H., and Ng, N. L.: Influence of seed aerosol surface area and oxidation rate on vapor wall deposition and SOA mass yields: a case study with α-pinene ozonolysis, Atmos. Chem. Phys., 16, 9361-9379, https://doi.org/10.5194/acp-16-9361-2016, 2016.

Nah, T., McVay, R. C., Pierce, J. R., Seinfeld, J. H., and Ng, N. L.: Constraining uncertainties in particle-wall deposition correction during SOA formation in chamber experiments, Atmos. Chem. Phys., 17, 2297-2310, https://doi.org/10.5194/acp-17-2297-2017, 2017.

Zhang, X., Schwantes, R. H., McVay, R. C., Lignell, H., Coggon, M. M., Flagan, R. C., and Seinfeld, J. H.: Vapor wall deposition in Teflon chambers, Atmos. Chem. Phys., 15, 4197-4214, https://doi.org/10.5194/acp-15-4197-2015, 2015.

We agree with the reviewer that seed aerosols can promote the condensation of SOA-forming vapors onto seed aerosol instead of the chamber walls. However, inorganic salt can both participate into the SOA formation and change the reaction environment such as providing acidic surface and aqueous environment. These properties of seed aerosols probably interfere with the RH effect on SOA formation, as the RH combined with seed aerosols complicate the *m*-xylene-OH system. Losses of organic vapors to the chamber wall can be substantial. The fact that seed aerosols were not artificially introduced can probably lead to the underestimation of SOA. Thus, we have added a paragraph to comment on how vapor wall loss affects our results at the end of Sec. 3.1 in the revised manuscript, but we cannot provide a factor of underestimation of SOA yields.

It should be noted that seed aerosols were not artificially introduced throughout all the experiments, which could lead to the underestimation of SOA, as SOA-forming vapors partly condense to the chamber walls instead of particles (Matsunaga and Ziemann, 2010; Zhang et al., 2014). The extent to which vapor wall deposition affects SOA mass yields depends on the specific parent hydrocarbon system (Zhang et al., 2014; Zhang et al., 2015; Nah et al., 2016; Nah et al., 2017). Zhang et al (2014) have estimated two *m*-xylene systems under low NO_x conditions and concluded that SOA mass yields were underestimated by factors of 1.8 (Ng et al., 2007) and 1.6 (Loza et al., 2012) under low RH conditions. In addition, the excess use of H_2O_2 can lead to an excess OH radicals, leading to a less underestimation of SOA formation as the losses of SOA-forming vapors can be mitigated via the use of excess oxidant concentrations (Nah et al., 2016). Thus, the underestimation of SOA formation can be limited. In fact, the wall loss of *m*-xylene was not taken into consideration of calculation of mass yields, which generally overestimates the mass yields.

Loza, C. L., Chhabra, P. S., Yee, L. D., Craven, J. S., Flagan, R. C., and Seinfeld, J. H.: Chemical aging of m-xylene secondary organic aerosol: laboratory chamber study, Atmos. Chem. Phys., 12, 151-167, 10.5194/acp-12-151-2012, 2012.

Matsunaga, A., and Ziemann, P. J.: Gas-wall partitioning of organic compounds in a Teflon film chamber and potential effects on reaction product and aerosol yield measurements, Aerosol Sci. Technol., 44, 881-892, 10.1080/02786826.2010.501044, 2010.

Nah, T., McVay, R. C., Zhang, X., Boyd, C. M., Seinfeld, J. H., and Ng, N. L.: Influence of seed aerosol surface area and oxidation rate on vapor wall deposition and SOA mass yields: a case study with α-pinene ozonolysis, Atmos. Chem. Phys., 16, 9361-9379, 10.5194/acp-16-9361-2016, 2016.

Nah, T., McVay, R. C., Pierce, J. R., Seinfeld, J. H., and Ng, N. L.: Constraining uncertainties in particle-wall deposition correction during SOA formation in chamber experiments, Atmos. Chem. Phys., 17, 2297-2310, 10.5194/acp-17-2297-2017, 2017.

Ng, N. L., Kroll, J. H., Chan, A. W. H., Chhabra, P. S., Flagan, R. C., and Seinfeld, J. H.: Secondary organic aerosol formation from m-xylene, toluene, and benzene, Atmos. Chem. Phys., 7, 3909-3922, 10.5194/acp-7-3909-2007, 2007.

Zhang, X., Cappa, C. D., Jathar, S. H., McVay, R. C., Ensberg, J. J., Kleeman, M. J., and Seinfeld, J. H.: Influence of vapor wall loss in laboratory chambers on yields of secondary organic aerosol, Proc. Natl. Acad. Sci. U. S. A., 111, 5802-5807, 10.1073/pnas.1404727111, 2014.

3. Page 4 line 11: How were the particle wall loss rates determined? In seed aerosols only experiments? Were these particle wall loss rates measured by tracking the decay of the aerosol mass or volume? How often were particle wall loss experiments conducted? Were the reported particle wall loss rates consistent with previously measured rates? Was the particle wall loss rate always faster in high RH experiments or is this measurement within experimental uncertainty?

Particle wall loss rates were generally measured in seed aerosol experiments by tracking the decay of the aerosol volume. For the same volume of new reactor, the wall loss rates were evaluated. We also checked the wall loss rate for the old reactor. Particle wall loss rate constant varies from 3×10^{-5} s^{-1} to 6×10^{-5} s^{-1} at the RH range of 5% to 90% with a trend of increase with RH, but their relationship is not statistically significant. The average particle wall loss rate constant is $(3.8 \pm 0.8) \times 10^{-5}$ s^{-1} at (13 ± 10)% RH and $(4.2 \pm 1.8) \times 10^{-5}$ s^{-1} at (79 ± 10)% RH, respectively. The relatively large wall loss rate at high RH and small wall loss rate at low RH are used in our correction of particle wall loss to look at RH effects in this study.

4. Page 4 line 14: It is not clear how the aerosol LWC was calculated. More details should be provided.

Taking the reviewer's advice, we have added some sentences about the details of LWC measurement at the end of the first paragraph of Sec. 2.2.

Thus, here a brief introduction is only given. After the lights were turned off in high RH experiments, the SMPS was modified to the dry mode through adding a Nafion dryer (Perma Pure MD-700-12F-3) to the sampling flow and a Nafion dryer (Perma Pure PD-200T-24MPS) to the sheath flow, leading to the reduction of RH in the sample air to 10 % and that in the sheath to 7 %. After modifying to the dry mode, the humid air in SMPS was quickly replaced by dry air through venting the sheath air at 5 L min^{-1}, and then the dry aerosol was measured by SMPS. The LWC was determined by the difference of the particle mass concentrations before and after the modification of the dry mode.

5. Page 4 line 20: The PILS only samples water-soluble species in the SOA, not the total SOA composition. Hence, the compositional results reported by the authors in this study are really the water-soluble species, and the authors should specify this in their manuscript. On a related note, why did the authors decided to collect aerosol samples with a PILS instead of on filters. Filter collection and analysis would have allowed them to analyze both the water-soluble and water-insoluble species. Do the authors know what fraction of the SOA formed is composed of water-soluble vs. water-insoluble species?

We agree with the reviewer that the PILS samples water-soluble species in the SOA. Nevertheless, after the FTIR measurement of SOA samples collected on ZnSe windows, the ZnSe window was washed with ultrapure water and was measured by FTIR again, no absorbance was observed on FTIR spectra. It can be believed that the SOA compositions are almost all water-soluble species and the PILS samples almost all SOA components. In addition, we agree with the reviewer that filter collection samples both water-soluble and water-insoluble species in the SOA. However, the filter-based analysis has its limitation, including adsorption of organic vapors and evaporation of semi-volatile organic compounds from the filter surface, leading to some uncertainties in the identification of SOA components. Moreover, Bateman et al. (2010) compared the off-line mass spectra of SOA samples from limonene ozonolysis collected by PILS with those collected on filters and found that the peak abundance, organic mass to organic carbon ratios, and the average O:C ratio are essentially identical. Water-soluble species account for the vast majority of SOA.

Bateman, A. P., Nizkorodov, S. A., Laskin, J., and Laskin, A.: High-resolution electrospray ionization mass spectrometry analysis of water-soluble organic aerosols collected with a particle into liquid sampler, Anal. Chem., 82, 8010-8016, 10.1021/ac1014386, 2010.

6. Page 5 line 8: Show the corresponding reaction time profile of m-xylene measured by the GC-MS that accompanied the observed SOA growth for the four experiments. This can be placed in the supplementary information. It is currently unclear how quickly the reactions took place. Perhaps the time profiles can be used to explain the differences in SOA formation in dry vs. humid conditions? For example, did m-xylene react faster in the dry experiments thus resulting in higher SOA mass yields? Ng et al., ACP 2007 previously showed that SOA formation in the m-xylene system will be faster at faster oxidation rates. From Fig. 1, it looks like peak SOA growth was not achieved at the end of the dry experiments (SOA mass looks like it may still increase). Why the authors decide to stop these dry experiments early? Won’t that affect their calculated SOA mass yields?

Ng, N. L., Kroll, J. H., Chan, A. W. H., Chhabra, P. S., Flagan, R. C., and Seinfeld, J. H.: Secondary organic aerosol formation from m-xylene, toluene, and benzene, Atmos. Chem. Phys., 7, 3909-3922, https://doi.org/10.5194/acp-7-3909-2007, 2007.

Taking the reviewer's advice, we have added the reaction time profile of *m*-xylene measured by the GC-MS that accompanied the observed SOA growth for the four experiments in the supplementary information (see Fig. S1).

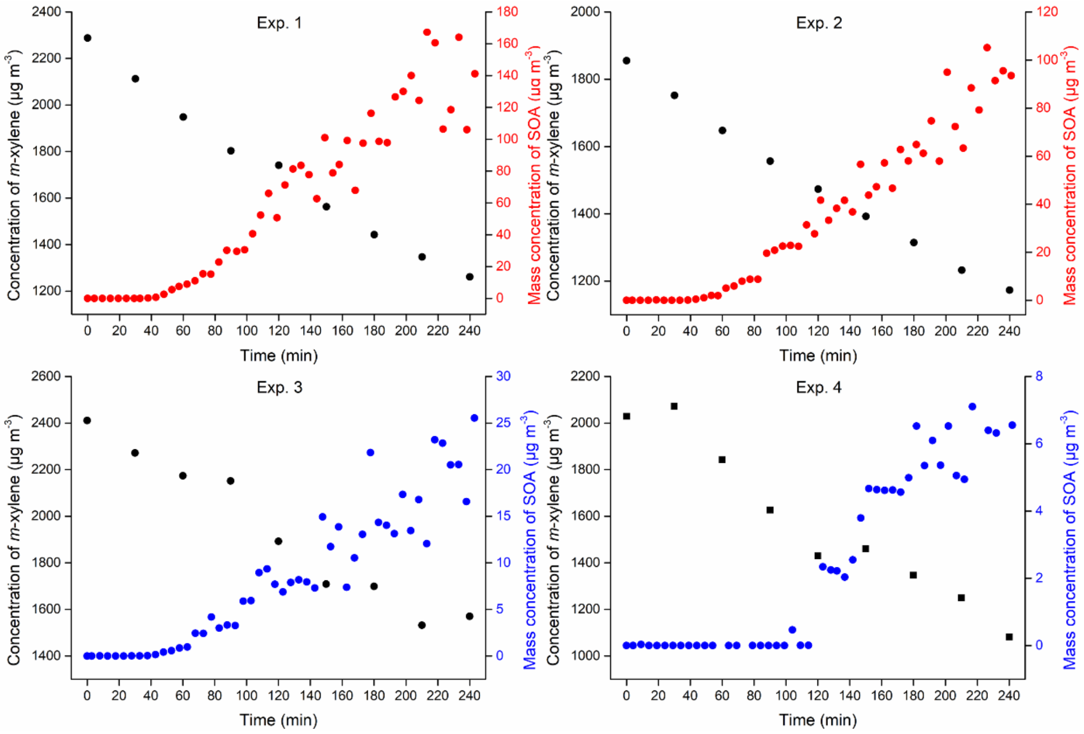

Fig. S1. Reaction time profiles of *m*-xylene measured by the GC-MS that accompanied the observed SOA growth for the four experiments

As shown in the time profile in Fig. S1, the reacted *m*-xylene account for around 40% of the initial *m*-xylene in both high and low RH experiments. *m*-Xylene did not react faster in the dry experiments, so that the oxidation rates were close at low and high RHs. Thus, the faster SOA formation at low RH cannot be explained with the oxidation rate (Ng et al, 2007).

As the reviewer pointed out, peak SOA growth was not achieved at the end of the dry experiments from Fig. 1 and SOA mass still increase. As the experiments were conducted under low NO_x condition, the SOA mass would increase unless all *m*-xylene reacted. The experiment for 4-6 h is a ubiquitous reaction time used in many previous studies. Indeed, the SOA yield generally increases with time. If the relationship between the yield and time is extrapolated to 6 h, the yield is increased by 45% relative to that at 4 h (Exp. 1), which can be compared with many previous studies (Cao and Jang, 2010; Hinks et al., 2018). Most importantly, as the purpose of our study is to investigate the RH effect on SOA formation, the reaction time of 4 h is sufficient to compare the SOA formation and to sample for SOA component analysis. Furthermore, a relatively short reaction time can minimize the wall loss of oxidized species and limit the further SOA mass uncertainty.

Cao, G., and Jang, M.: An SOA model for toluene oxidation in the presence of inorganic aerosols, Environ. Sci. Technol., 44, 727-733, 10.1021/es901682r, 2010.

Hinks, M. L., Montoya-Aguilera, J., Ellison, L., Lin, P., Laskin, A., Laskin, J., Shiraiwa, M., Dabdub, D., and Nizkorodov, S. A.: Effect of relative humidity on the composition of secondary organic aerosol from the oxidation of toluene, Atmos. Chem. Phys., 18, 1643-1652, 10.5194/acp-18-1643-2018, 2018.

Ng, N. L., Kroll, J. H., Chan, A. W. H., Chhabra, P. S., Flagan, R. C., and Seinfeld, J. H.: Secondary organic aerosol formation from *m*-xylene, toluene, and benzene, Atmos. Chem. Phys., 7, 3909-3922, 10.5194/acp-7-3909-2007, 2007.

7. Page 5 line 21: Regarding the authors’ definition of SOA yield, did they calculate the SOA yield by dividing the SOA mass obtained at the end of the experiment by the total reacted m-xylene at the end of the experiment? If yes, why did they decide to use this calculation? Previous chamber studies calculated the SOA mass yield by taking the ratio of the SOA mass at peak SOA mass divided by the mass of VOC reacted. Was peak SOA mass only reached at the end of each experiment (reaction time profiles of SOA mass growth with the corresponding reacted m-xylene for the four experiments will be useful; see comment 6)? Related to this point, are the authors confident that peak SOA mass have already occurred before they ended their experiment. Given that the authors are comparing their measured SOA mass yields with previous studies, they should make sure that their calculation of SOA mass yields are consistent with those of previous studies before they compare mass yields.

Yes, the reviewer is right that the SOA yield in our study is defined by the ratio of the SOA mass obtained at the end of the experiment to the total reacted m-xylene at the end of the experiment. The further questions about peak SOA mass, time profiles, comparison with previous studies, etc. in Comment 7 have been replied in Comment 6 together.

8. Page 5 line 23: How was LWC subtracted from the SOA measurement? How did the authors determine the amount of LWC in the aerosols? The authors should briefly describe this process even if this was previously mentioned in one of their previous paper. The sentence “It should be pointed out that...would evaporate back into the gas phase when aerosol water is removed” is confusing. The experimental section did not mention that authors removed aerosol water prior to SMPS measurement. If aerosol water was not removed prior to SMPS measurement, then this sentence seems out of place. Unless the authors are proposing a hypothetical situation?

Taking the reviewer’s advice, we have added some sentences about the details of LWC measurement at the end of the first paragraph of Sec. 2.2 (same with the reply of Comment 4).

Thus, here a brief introduction is only given. After the lights were turned off in high RH experiments, the SMPS was modified to the dry mode through adding a Nafion dryer (Perma Pure MD-700-12F-3) to the sampling flow and a Nafion dryer (Perma Pure PD-200T-24MPS) to the sheath flow, leading to the reduction of RH in the sample air to 10 % and that in the sheath to 7 %. After modifying to the dry mode, the humid air in SMPS was quickly replaced by dry air through venting the sheath air at 5 L min^{-1}, and then the dry aerosol was measured by SMPS. The LWC was determined by the difference of the particle mass concentrations before and after the modification of the dry mode.

When we measured the LWC, the aerosol water should be removed after the SMPS was modified. For clarification, we have rephrased the sentence pointed out by the reviewer, "The removal of aerosol water during the LWC measurement may cause the dissolved species that are probably volatile/semi-volatile compounds to evaporate back into the gas phase. Thus, SOA concentrations for high RH conditions were slightly underestimated, but the underestimation is extremely low and can be negligible."

9. Page 5 line 27: Table 1 should also state the m-xylene concentration in ug/m^3 so that readers can more easily compare this study's reaction conditions with those of previous studies.

Taking the reviewer's advice, we have modified the m-xylene concentration in μg/m^3 in Table 1.

Table 1. Experimental conditions, SOA concentrations and yields at the end of the experiments in *m*-xylene-OH oxidation system.

Exp. No.	[*m*-xylene]$_0$ (μg m^{-3})	[*m*-xylene]$_{reacted}$ (μg m^{-3})	RH (%)	T (°C)	[SOA]$_e$ (μg m^{-3})	SOA yield (%)
1	2287.9	1026.3	13.6	25.9	150.3 ± 15.0	14.6 ± 1.5
2	1855.5	682.0	13.7	25.3	95.5 ± 9.5	14.0 ± 1.4
3	2410.8	941.4	73.6	27.5	21.0 ± 2.1	2.2 ± 0.2
4	2029.1	946.9	79.1	27.4	7.5 ± 0.7	0.8 ± 0.1

[SOA]$_e$ indicates the mass concentration of SOA at the end of each experiment with particle wall loss corrected.

10. Page 5 line 28: Why were the temperatures in the high RH experiments higher than those in the low RH experiments?

The accuracy of temperature controller led to this fluctuation that the temperatures in the high RH experiments were higher than those in the low RH experiments. The highest difference between low and high RH experiment was 2°C. The temperature effect on SOA formation has been investigated in some previous studies about the *m*-xylene oxidation.

According to previous studies about the temperature effect of SOA formation from m-xylene oxidation (Takekawa et al., 2003; Qi et al., 2010), an increase of 2°C can lead to a mean SOA mass decrease by 4.6%. It can be concluded that the 2°C higher temperature in high RH experiments cannot significantly affect the results of RH effect on SOA formation in this study.

Qi, L., Nakao, S., Tang, P. and Cocker, D. R., III: Temperature effect on physical and chemical properties of secondary organic aerosol from m-xylene photooxidation, Atmos. Chem. Phys., 10, 3847-3854, 10.5194/acp-10-3847-2010, 2010.

Takekawa, H., Minoura, H. and Yamazaki, S.: Temperature dependence of secondary organic aerosol formation by photo-oxidation of hydrocarbons, Atmos. Environ., 37, 3413-3424, 10.1016/s1352-2310(03)00359-5, 2003.

11. page 7 line 25: A magnified view of the mass spectra shown in Fig. 3 would be more useful for comparison purposes.

Taking the reviewer's suggestion, we have magnified the view of the mass spectra shown in Fig. 3.

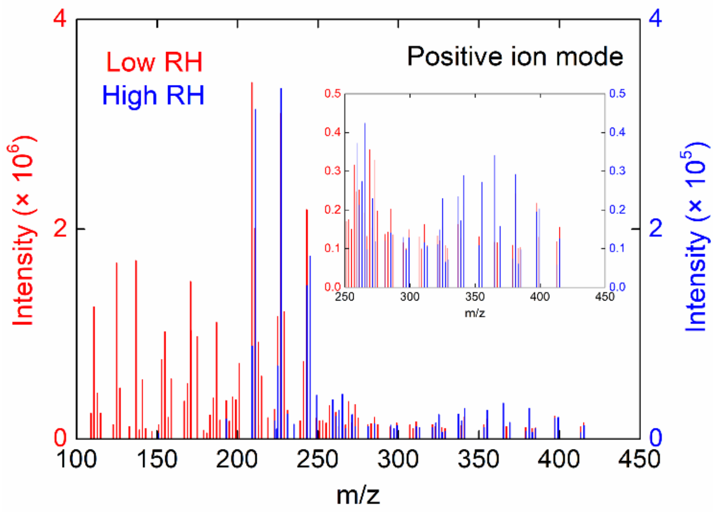

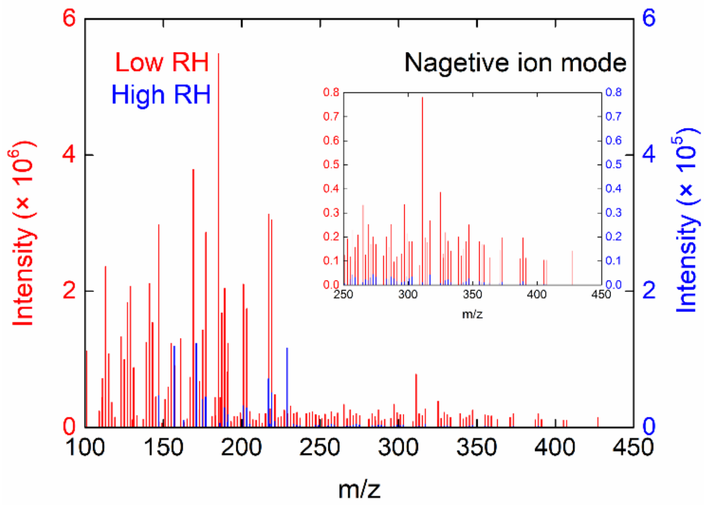

Figure 3. Selected background-subtraction HESI-Q Exactive-Orbitrap MS results of SOA in both positive and negative ion modes from the photooxidation of *m*-xylene-OH under both low and high RH conditions (Note that the Y-axis scales for low and high RH are largely different, 10^6 at low RH and 10^5 at high RH).

12. Page 7 line 27: The sentence "It should be pointed out that the signal intensities…" is confusing. Were the mass spectra for the different experiments obtained using different MS operation conditions (e.g., ESI spray conditions, MS collision gas)?

The sentence pointed out by the reviewer is indeed confusing and thus we have deleted this sentence in the text. The mass spectra for the different experiments were obtained using exactly same MS operation conditions. Thus, the mass spectra for different experiments were comparable.

13. Page 7 line 25 to page 8 line 11: The mass peaks discussed here do not seem to be the major peaks shown in Fig. 3. Why did the authors choose to focus their discussion only on these selected peaks? The major peaks seem to be m/z > 200. How were these products formed? The authors should include a list of all the product ions identified. Do these identified products match their proposed reaction mechanism show in Scheme 1?

The mass peaks discussed between Page 7 line 25 to page 8 line 11 are the most abundant peaks in Fig 3, so we gave the proposed structures and discussed here. The m/z > 200 peaks are not discussed in this paragraph, but we discussed the m/z > 200 peaks and explained how these products formed in the Sec 3.4. In addition, taking the reviewer's advice, we have added a list of all the product ions identified in Table S1 in the supplementary information. These identified products that match their proposed reaction mechanism shown in Scheme 1 are marked in Scheme 1.

Table S1(a). List of all the SOA product ions identified from ESI-HRMS in positive mode.

Low RH		High RH		Formula
m/z	intensity	m/z	intensity	
415.12032	1.55E+05	415.11937	1.26E+04	$C_{18}H_{23}O_{11}$
413.10459	1.18E+05	413.10393	5.79E+03	$C_{18}H_{21}O_{11}$
399.12542	1.30E+05	399.12470	2.03E+04	$C_{18}H_{23}O_{10}$
397.10976	2.18E+05	397.10926	1.95E+04	$C_{18}H_{21}O_{10}$
381.11482	2.42E+05	381.11434	2.92E+04	$C_{18}H_{21}O_{9}$
379.09902	1.09E+05	379.09866	7.43E+03	$C_{18}H_{19}O_{9}$
365.11992	1.17E+05	365.11944	3.41E+04	$C_{18}H_{21}O_{8}$
385.10957	1.03E+05	385.10901	9.72E+03	$C_{17}H_{21}O_{10}$
383.09399	1.01E+05	383.09330	6.04E+03	$C_{17}H_{19}O_{10}$
369.11481	1.06E+05	369.11446	1.57E+04	$C_{17}H_{21}O_{9}$
367.09911	1.15E+05	367.09892	-	$C_{17}H_{19}O_{9}$
355.09919	1.88E+05	355.09870	2.72E+04	$C_{16}H_{19}O_{9}$
353.08352	1.31E+05	353.08319	1.08E+04	$C_{16}H_{17}O_{9}$
339.10481	1.27E+05	339.10408	1.72E+04	$C_{16}H_{19}O_{8}$
337.08857	1.62E+05	337.08800	2.34E+04	$C_{16}H_{17}O_{8}$
321.09386	1.33E+05	321.09328	1.11E+04	$C_{16}H_{17}O_{7}$
341.08370	2.11E+05	341.08322	2.89E+04	$C_{15}H_{17}O_{9}$
325.08882	1.54E+05	325.08817	2.30E+04	$C_{15}H_{17}O_{8}$
323.07306	1.22E+05	323.07263	1.49E+04	$C_{15}H_{15}O_{8}$
309.09403	9.96E+04	309.09236	-	$C_{15}H_{17}O_{7}$
307.07817	1.31E+05	307.08028	-	$C_{15}H_{15}O_{7}$
329.08383	1.01E+05	329.08320	7.12E+03	$C_{14}H_{17}O_{9}$
327.06797	1.08E+05	327.06751	6.51E+03	$C_{14}H_{15}O_{9}$
313.08917	1.08E+05	313.08830	1.05E+04	$C_{14}H_{17}O_{8}$
311.07309	1.62E+05	311.07260	1.15E+04	$C_{14}H_{15}O_{8}$
297.09553	9.65E+04	297.09353	9.68E+03	$C_{14}H_{17}O_{7}$
295.07852	1.11E+05	295.07782	1.29E+04	$C_{14}H_{15}O_{7}$
281.10079	8.07E+04	281.09867	-	$C_{14}H_{17}O_{6}$
299.07316	1.49E+05	299.07245	1.29E+04	$C_{13}H_{15}O_{8}$
297.05750	9.95E+04	297.05697	7.39E+03	$C_{13}H_{13}O_{8}$

283.07818	1.43E+05	283.07558	-	C13 H15 O7
281.06267	1.37E+05	281.06220	1.19E+04	C13 H13 O7
267.08471	1.06E+05	267.08299	-	C13 H15 O6
265.06795	9.57E+04	265.06732	1.06E+04	C13 H13 O6
287.07312	1.36E+05	287.07266	-	C12 H15 O8
285.05754	2.03E+05	285.05710	1.41E+04	C12 H13 O8
271.07849	1.33E+05	271.07786	2.30E+04	C12 H15 O7
269.06262	3.57E+05	269.06157	-	C12 H13 O7
267.04693	1.32E+05	267.04613	9.73E+03	C12 H11 O7
265.02894	1.92E+05	265.02852	4.24E+04	C12 H9 O7
263.01347	1.17E+05	263.01304	2.73E+04	C12 H7 O7
255.08462	8.73E+04	255.08340	-	C12 H15 O6
253.06787	1.75E+05	253.06731	-	C12 H13 O6
251.05217	1.70E+05	251.05172	-	C12 H11 O6
249.03409	1.97E+05	249.03366	4.15E+04	C12 H9 O6
231.02374	1.62E+05	231.02326	2.38E+04	C12 H7 O5
275.07311	1.97E+05	275.07260	-	C11 H15 O8
273.05759	3.28E+05	273.05718	1.18E+04	C11 H13 O8
271.04182	1.54E+05	271.04129	6.63E+03	C11 H11 O8
259.07844	2.48E+05	259.07786	3.72E+04	C11 H15 O7
257.06264	3.15E+05	257.06224	-	C11 H13 O7
255.04708	1.51E+05	255.04659	-	C11 H11 O7
243.08360	2.76E+05	243.08304	5.15E+04	C11 H15 O6
239.05231	1.71E+05	239.05191	-	C11 H11 O6
235.01848	9.71E+04	235.01853	1.38E+04	C11 H7 O6
225.07285	1.87E+05	225.07253	-	C11 H13 O5
223.05754	8.06E+04	223.05702	-	C11 H11 O5
261.05771	2.51E+05	261.05727	2.13E+04	C10 H13 O8
259.04210	1.99E+05	259.04157	8.26E+03	C10 H11 O8
245.06288	1.36E+06	245.06243	1.74E+05	C10 H13 O7
243.04720	2.19E+06	243.04677	1.46E+05	C10 H11 O7
241.03138	7.38E+05	241.02850	-	C10 H9 O7
229.06802	1.21E+06	229.06751	-	C10 H13 O6

227.05224	3.10E+06	227.05182	3.34E+05	C10 H11 O6
225.03667	1.16E+06	225.03624	6.95E+04	C10 H9 O6
223.01851	2.82E+05	223.01812	1.69E+04	C10 H7 O6
213.07305	1.30E+05	213.07248	-	C10 H13 O5
211.05741	2.01E+06	211.05702	3.14E+05	C10 H11 O5
209.04177	3.40E+06	209.04141	8.84E+04	C10 H9 O5
193.04693	3.66E+05	193.04652	-	C10 H9 O4
181.08606	5.51E+04	181.08581	-	C10 H13 O3
179.07026	6.43E+04	179.06998	-	C10 H11 O3
231.04717	2.73E+05	231.04688	1.32E+04	C9 H11 O7
229.03161	1.01E+05	229.03122	-	C9 H9 O7
215.05216	5.96E+05	215.05182	-	C9 H11 O6
213.03667	9.22E+05	213.03617	-	C9 H9 O6
199.05730	3.73E+05	199.05692	-	C9 H11 O5
197.04179	4.02E+05	197.04137	-	C9 H9 O5
195.02624	1.68E+05	195.02591	-	C9 H7 O5
193.00815	3.16E+05	193.00767	1.88E+04	C9 H5 O5
185.08084	1.38E+05	185.07750	-	C9 H13 O4
183.06534	1.05E+05	183.06212	-	C9 H11 O4
179.03120	8.18E+04	179.03112	-	C9 H7 O4
167.07030	1.20E+05	167.06986	-	C9 H11 O3
147.05008	7.10E+04	147.04975	-	C9 H7 O2
201.03665	7.21E+05	201.03628	-	C8 H9 O6
189.07567	1.76E+05	189.07240	-	C8 H13 O5
187.06003	1.11E+06	187.05678	-	C8 H11 O5
185.04165	3.88E+05	185.04139	-	C8 H9 O5
183.02618	2.25E+05	183.02609	-	C8 H7 O5
171.06509	1.03E+06	171.06488	-	C8 H11 O4
169.04959	5.29E+05	169.04638	-	C8 H9 O4
167.03115	3.59E+05	167.03077	-	C8 H7 O4
155.07013	1.02E+06	155.06985	-	C8 H11 O3
153.05453	7.56E+05	153.05425	-	C8 H9 O3
151.03891	1.33E+05	151.03874	4.89E+03	C8 H7 O3

137.05962	1.70E+06	137.05931	-	C8 H9 O2
219.01631	2.01E+05	219.01588	-	C7 H7 O8
189.03670	1.66E+05	189.03673	-	C7 H9 O6
171.03328	1.50E+06	171.03295	-	C7 H7 O5
171.02640	2.77E+05	171.02571	-	C7 H7 O5
157.04949	2.03E+05	157.04906	-	C7 H9 O4
155.03117	8.61E+04	155.03096	-	C7 H7 O4
141.05445	5.63E+05	141.05420	-	C7 H9 O3
139.03886	8.46E+04	139.03859	-	C7 H7 O3
125.05974	1.68E+06	125.05950	-	C7 H9 O2
123.04411	1.34E+05	123.04389	-	C7 H7 O2
109.06503	2.41E+05	109.06480	-	C7 H9 O
209.02861	6.79E+04	209.02812	-	C6 H9 O8
175.03264	1.17E+05	175.03264	-	C6 H7 O6
175.02542	9.74E+05	175.02510	-	C6 H7 O6
157.01758	8.63E+04	157.01737	-	C6 H5 O5
143.03380	9.78E+04	143.03354	-	C6 H7 O4
127.03897	4.85E+05	127.03868	-	C6 H7 O3
113.05988	4.34E+05	113.05967	-	C6 H9 O2
111.04425	1.26E+06	111.04405	-	C6 H7 O2
215.03908	9.91E+04	215.03895	-	C5 H11 O9
199.04426	7.18E+04	199.04416	-	C5 H11 O8
115.03911	2.47E+05	115.03889	-	C5 H7 O3

Table S1(b). List of all the SOA product ions identified from ESI-HRMS in negative mode.

Low RH		High RH		Formula
m/z	Intensity	m/z	Intensity	
309.17388	8.22E+04	309.17346	-	C17 H25 O5
427.02033	1.43E+05	427.01930	3.35E+02	C16 H11 O14
407.11955	1.04E+05	407.11842	2.19E+02	C16 H23 O12
405.10387	1.04E+05	405.10320	2.63E+02	C16 H21 O12
391.12466	1.12E+05	391.12383	2.93E+02	C16 H23 O11
389.10906	1.96E+05	389.10828	1.48E+03	C16 H21 O11

387.09325	1.09E+05	387.09280	5.09E+02	C16 H19 O11
373.11399	1.97E+05	373.11329	1.26E+03	C16 H21 O10
371.09821	1.44E+05	371.09766	6.70E+02	C16 H19 O10
357.11903	1.69E+05	357.11856	9.95E+02	C16 H21 O9
355.10338	1.80E+05	355.10274	1.62E+03	C16 H19 O9
359.09835	1.67E+05	359.09778	1.15E+03	C15 H19 O10
343.10330	1.50E+05	343.10278	1.01E+03	C15 H19 O9
341.08758	1.21E+05	341.08664	5.45E+02	C15 H17 O9
339.20000	2.00E+05	339.19922	-	C15 H31 O8
327.10844	1.12E+05	327.10799	5.27E+02	C15 H19 O8
325.09285	1.08E+05	325.09217	6.23E+02	C15 H17 O8
265.14792	3.33E+05	265.14776	-	C15 H21 O4
218.03824	2.71E+05	218.03779	5.27E+03	C15 H6 O2
363.09335	1.13E+05	363.09077	9.01E+02	C14 H19 O11
347.09836	2.51E+05	347.09758	2.67E+03	C14 H19 O10
345.08263	1.80E+05	345.08202	1.35E+03	C14 H17 O10
331.10347	1.83E+05	331.10283	2.34E+03	C14 H19 O9
329.08781	2.19E+05	329.08696	1.87E+03	C14 H17 O9
327.07190	1.29E+05	327.07119	9.89E+02	C14 H15 O9
325.18438	3.85E+05	325.18366	-	C14 H29 O8
313.09287	1.96E+05	313.09204	1.88E+03	C14 H17 O8
311.07715	1.52E+05	311.07670	1.01E+03	C14 H15 O8
297.09786	1.32E+05	297.09724	1.05E+03	C14 H17 O7
295.08212	1.29E+05	295.08163	9.81E+02	C14 H15 O7
333.08273	1.42E+05	333.08206	1.23E+03	C13 H17 O10
331.06692	9.75E+04	331.06613	7.28E+02	C13 H15 O10
317.08774	2.67E+05	317.08714	4.21E+03	C13 H17 O9
315.07210	1.77E+05	315.07401	-	C13 H15 O9
311.16878	7.80E+05	311.16806	-	C13 H27 O8
301.09273	1.82E+05	301.09215	2.77E+03	C13 H17 O8
299.07727	2.15E+05	299.07641	3.44E+03	C13 H15 O8
297.06154	1.09E+05	297.06002	1.42E+03	C13 H13 O8
285.09789	1.00E+05	285.09726	1.77E+03	C13 H17 O7

283.08221	2.00E+05	283.08162	2.54E+03	C13 H15 O7
281.06697	1.22E+05	281.06609	-	C13 H13 O7
267.08726	1.26E+05	267.08657	2.19E+03	C13 H15 O6
265.07197	1.61E+05	265.07106	1.19E+03	C13 H13 O6
247.06280	1.81E+05	247.06092	3.33E+02	C13 H11 O5
231.06771	3.10E+05	231.06592	-	C13 H11 O4
303.07184	1.82E+05	303.07152	3.35E+03	C12 H15 O9
301.05629	9.34E+04	301.05576	1.42E+03	C12 H13 O9
297.15292	3.35E+05	297.15230	-	C12 H25 O8
287.07698	2.52E+05	287.07691	3.35E+03	C12 H15 O8
285.06133	1.57E+05	285.06109	2.27E+03	C12 H13 O8
271.08217	1.69E+05	271.08173	3.03E+03	C12 H15 O7
269.06606	2.53E+05	269.06611	2.03E+03	C12 H13 O7
267.05024	9.81E+04	267.05010	7.33E+02	C12 H11 O7
255.08719	1.17E+05	255.08664	-	C12 H15 O6
253.07111	1.91E+05	253.07089	-	C12 H13 O6
251.05515	1.24E+05	251.05505	5.59E+02	C12 H11 O6
237.07648	1.36E+05	237.07600	-	C12 H13 O5
221.08136	8.88E+04	221.08108	-	C12 H13 O4
291.07203	1.18E+05	291.07139	1.57E+03	C11 H15 O9
289.05636	9.61E+04	289.05566	2.67E+03	C11 H13 O9
275.07729	1.70E+05	275.07673	3.31E+03	C11 H15 O8
273.06161	2.00E+05	273.06105	4.47E+03	C11 H13 O8
259.08219	1.57E+05	259.08171	3.21E+03	C11 H15 O7
257.06651	2.28E+05	257.06598	4.31E+03	C11 H13 O7
255.05088	1.07E+05	255.05025	2.48E+03	C11 H11 O7
243.08714	8.57E+04	243.08664	-	C11 H15 O6
241.07147	2.04E+05	241.07093	-	C11 H13 O6
225.07641	1.52E+05	225.07596	-	C11 H13 O5
223.06071	1.40E+05	223.06018	-	C11 H11 O5
209.08133	1.02E+05	209.08102	-	C11 H13 O4
207.06573	1.11E+05	207.06531	-	C11 H11 O4
193.08630	7.02E+04	193.08600	-	C11 H13 O3

261.06155	2.09E+05	261.05977	-	C10 H13 O8
259.04588	9.74E+04	259.04511	3.26E+03	C10 H11 O8
245.06644	2.22E+05	245.06586	-	C10 H13 O7
243.05084	2.08E+05	243.05037	-	C10 H11 O7
229.07132	2.03E+05	229.07087	-	C10 H13 O6
227.05570	2.51E+05	227.05525	-	C10 H11 O6
211.06064	1.96E+05	211.06027	-	C10 H11 O5
209.04512	9.50E+04	209.04452	-	C10 H9 O5
195.06563	1.61E+05	195.06536	-	C10 H11 O4
193.05002	8.88E+04	193.04978	-	C10 H9 O4
181.08628	9.12E+04	181.08592	-	C10 H13 O3
163.07558	5.18E+04	163.07520	-	C10 H11 O2
249.06096	1.71E+05	249.06092	2.65E+03	C9 H13 O8
247.04556	1.43E+05	247.04500	3.44E+03	C9 H11 O8
233.06614	1.99E+05	233.06580	4.43E+03	C9 H13 O7
231.05066	1.62E+05	231.05023	-	C9 H11 O7
229.03504	7.84E+04	229.03443	-	C9 H9 O7
217.07129	1.69E+05	217.07080	-	C9 H13 O6
215.05569	2.04E+05	215.05511	-	C9 H11 O6
201.07618	2.38E+05	201.07580	-	C9 H13 O5
199.06058	1.95E+05	199.06031	-	C9 H11 O5
197.04500	1.59E+05	197.04464	-	C9 H9 O5
183.06553	1.70E+05	183.06531	-	C9 H11 O4
181.04989	1.64E+05	181.04952	-	C9 H9 O4
165.05484	1.21E+05	165.05454	-	C9 H9 O3
149.05981	6.31E+04	149.05947	-	C9 H9 O2
237.06126	9.92E+04	237.06075	2.61E+03	C8 H13 O8
235.04566	2.21E+05	235.04511	2.88E+03	C8 H11 O8
233.03005	1.23E+05	233.02891	-	C8 H9 O8
221.06623	4.82E+05	221.06579	8.46E+03	C8 H13 O7
219.05057	3.05E+06	219.05011	5.02E+04	C8 H11 O7
217.03488	3.13E+06	217.03444	7.13E+04	C8 H9 O7
205.07117	2.33E+05	205.07077	4.95E+03	C8 H13 O6

203.05550	1.74E+06	203.05513	2.87E+04	C8 H11 O6
201.03983	2.10E+06	201.03967	3.18E+04	C8 H9 O6
199.02428	2.08E+05	199.02409	-	C8 H7 O6
187.06049	1.68E+06	187.06013	-	C8 H11 O5
185.04483	5.49E+06	185.04449	-	C8 H9 O5
183.02923	4.41E+05	183.02901	-	C8 H7 O5
171.06543	5.43E+05	171.06511	1.23E+05	C8 H11 O4
169.04976	3.79E+06	169.04954	-	C8 H9 O4
167.03412	7.36E+05	167.03368	-	C8 H7 O4
153.05472	5.91E+05	153.05442	-	C8 H9 O3
151.03908	4.09E+05	151.03878	-	C8 H7 O3
137.05970	1.18E+05	137.05943	-	C8 H9 O2
205.03496	2.28E+05	205.03286	-	C7 H9 O7
191.05540	1.23E+06	191.05504	1.88E+04	C7 H11 O6
189.03975	2.04E+06	189.03942	2.91E+04	C7 H9 O6
187.02422	1.80E+05	187.02389	-	C7 H7 O6
175.06041	1.80E+05	175.06006	-	C7 H11 O5
173.04471	6.71E+05	173.04440	-	C7 H9 O5
171.02908	6.75E+05	171.02879	-	C7 H7 O5
169.01357	1.20E+05	169.01317	-	C7 H5 O5
157.04965	9.08E+05	157.04939	-	C7 H9 O4
155.03403	1.23E+06	155.03374	-	C7 H7 O4
153.01828	2.32E+05	153.01805	-	C7 H5 O4
141.05463	2.11E+06	141.05439	-	C7 H9 O3
139.03897	1.25E+06	139.03869	-	C7 H7 O3
125.05961	6.55E+05	125.05940	-	C7 H9 O2
123.04397	1.33E+06	123.04376	-	C7 H7 O2
229.05210	1.79E+05	229.04953	-	C6 H13 O9
213.05676	6.20E+04	213.05473	-	C6 H13 O8
191.01907	1.26E+05	191.01873	7.54E+03	C6 H7 O7
177.03967	2.86E+06	177.03930	4.45E+04	C6 H9 O6
175.02402	1.43E+06	175.02363	4.04E+04	C6 H7 O6
173.00836	2.54E+05	173.00529	-	C6 H5 O6

161.04464	1.30E+06	161.04430	-	C6 H9 O5
157.01330	3.67E+05	157.01334	-	C6 H5 O5
147.06522	8.02E+04	147.06492	-	C6 H11 O4
145.04957	3.71E+05	145.04929	-	C6 H9 O4
143.03391	1.54E+06	143.03365	-	C6 H7 O4
141.01827	7.79E+05	141.01797	-	C6 H5 O4
139.00264	6.12E+04	139.00224	-	C6 H3 O4
127.03890	1.83E+06	127.03866	-	C6 H7 O3
125.02325	9.93E+05	125.02297	-	C6 H5 O3
113.05952	7.21E+05	113.05925	-	C6 H9 O2
111.04388	7.15E+05	111.04361	-	C6 H7 O2
109.02824	2.35E+05	109.02805	-	C6 H5 O2
201.05694	1.09E+05	201.05479	-	C5 H13 O8
163.02399	7.06E+04	163.02364	1.05E+04	C5 H7 O6
147.02887	2.97E+06	147.02878	4.63E+04	C5 H7 O5
145.01320	4.46E+05	145.01289	-	C5 H5 O5
131.03383	8.78E+05	131.03360	-	C5 H7 O4
129.01819	2.07E+06	129.01793	-	C5 H5 O4
127.00253	1.97E+05	127.00232	-	C5 H3 O4
115.03882	1.08E+06	115.03858	-	C5 H7 O3
113.02311	2.36E+06	113.02278	-	C5 H5 O3
111.00750	4.41E+05	111.00726	-	C5 H3 O3
133.01316	1.69E+05	133.01282	-	C4 H5 O5
119.03381	1.48E+05	119.03355	-	C4 H7 O4
117.01807	3.64E+05	117.01775	-	C4 H5 O4
115.00245	3.19E+05	115.00215	-	C4 H3 O4
101.02308	1.11E+06	101.02289	-	C4 H5 O3

14: General comment: What compounds are the -ve MS mode sensitive to? Were these compounds identified in their collected mass spectra?

In positive mode analysis, ions are produced by protonation. Thus, groups that more readily accept a positive charge, such as carbonyls, are often observed in this mode. As listed in Table 3, the proposed compounds obtained by HRMS in positive ion mode are all with the carbonyl group. Negative mode analysis leads to formation of deprotonated ions. Thus, molecules containing functional groups that readily lose a proton, such as carboxylic acids, are frequently observed in this mode. Also, the esters compounds can be obtained in the negative ion mode (Hamilton et al., 2008; Camredon et al., 2010; Ge et al., 2017). In the MCM prediction about m-xylene-OH oxidation, many carbonyls are included. It can be deduced that many carboxylic acids can be formed via OH oxidation of these carbonyls and these carboxylic acids can be measured in the negative ion mode.

Camredon, M., Hamilton, J. F., Alam, M. S., Wyche, K. P., Carr, T., White, I. R., Monks, P. S., Rickard, A. R., and Bloss, W. J.: Distribution of gaseous and particulate organic composition during dark α-pinene ozonolysis, Atmos. Chem. Phys., 10, 2893-2917, 10.5194/acp-10-2893-2010, 2010.

Ge, S., Xu, Y. and Jia, L.: Secondary organic aerosol formation from propylene irradiations in a chamber study, Atmos. Environ., 157, 146-155, 10.1016/j.atmosenv.2017.03.019, 2017.

Hamilton, J. F., Lewis, A. C., Carey, T. J., and Wenger, J. C.: Characterization of polar compounds and oligomers in secondary organic aerosol using liquid chromatography coupled to mass spectrometry, Anal. Chem., 80, 474-480, 10.1021/ac701852t, 2008.

15. General comment: The authors mentioned in the experimental system that they used a HPLC-MS system in their study. It is not clear from their presented results whether this was the case. Was HPLC not used to separate the products via their volatilities prior to MS analysis?

HPLC was used in our experiments as the injection system before HRMS analysis. We used the high resolution of mass analyzer for the separation of major SOA components instead of HPLC.

16. Page 9 line 30: The authors claimed that they used the distribution of relative intensity of SOA products with the same carbon number to investigate the potential RH effect on HOMs. The rationale behind this course of action seems to contradict their previous statement in Page 7 line 27 that signal intensities can be biased by ionization properties.

The statement was incorrect and confusing in Page 7 Line 27 and we have deleted it from the text. The mass spectra for the different experiments were obtained using same MS operation conditions. Thus, the mass spectra for different experiments were comparable (see the reply of Comment 12).

17. Scheme 1: The authors should indicate explicitly in Scheme 1 which are the products that they have identified.

Taking the reviewer’s advice, we have modified Scheme 1 in which the products identified are marked with a molecular weight number below the molecular formula.

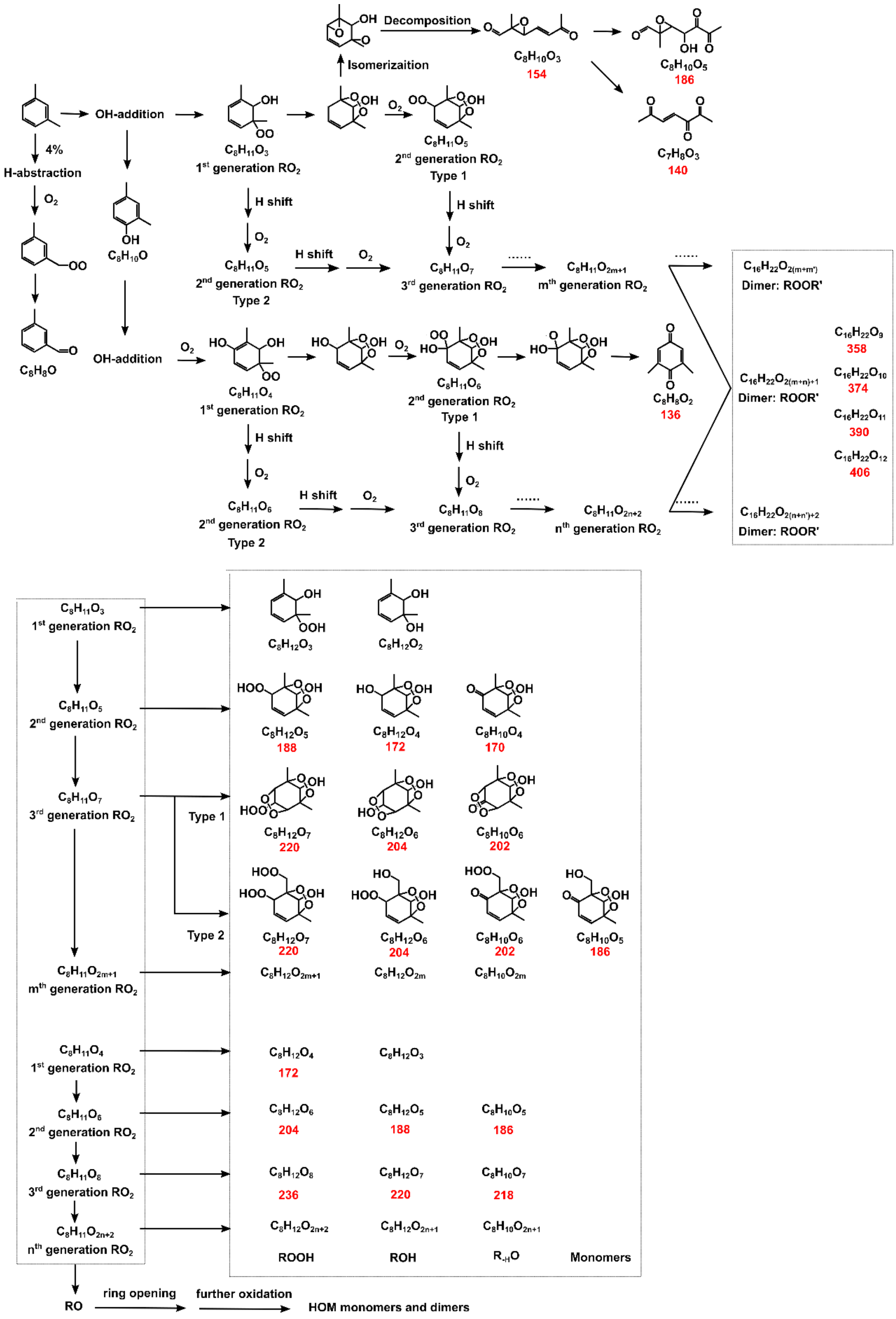

Scheme 1. The route of OH-initiated *m*-xylene oxidation. The red number below the molecular formula is its molecular weight, which is determined by HRMS to exist in the particle phase.

18. Page 10 line 27: The sentence “Together with the previous study on toluene SOA, it is conceivable that the effect of RH on SOA yield is a common feature of SOA formation from oxidation of all OH-initiated aromatics” is too generalized and needs to be rephrased. As discussed by the authors in their introduction, an increase RH does not necessarily cause a decrease in SOA mass yields in aromatics SOA systems. Other factors such as NOx can also alter the effect that RH has on SOA mass yields in these systems.

Taking the reviewer’s advice, we have rephrased the sentence in Page 10 line 27.

Together with the previous study on toluene SOA, it is conceivable that the effect of RH on SOA yield is a common feature of SOA formation from aromatics oxidation under low NO_x conditions and using H_2O_2 as the OH radical source.

Response to Reviewer 2

We greatly appreciate the time and effort that reviewer 2 spent in reviewing our manuscript. The comments are really thoughtful and helpful to improve the quality of our paper. Reviewer 2 has provided both main comments and other specific comments. Below we make a point-by-point response to these comments. According to editor's requirement, the response to the reviewer 2 is structured in the following sequence: (1) comments from the reviewer in black color, (2) our response in blue color, and (3) our changes in the revised manuscript in red color.

Overview:

This study explore the role of relative humidity (RH) on the m-xylene SOA formation under OH initiated no NOx condition. The results showed that the SOA yield under high RH is significantly lower than that under low RH conditions. This study provides SOA yields and particle-phase SOA products under different RH levels. The LWC was measured by the particles mass deduction in the DAASS. The authors measured the SOA compositions by using a Fourier transform infrared (FTIR) spectra and ultrahigh performance liquid chromatograph electrospray ionization-high-resolution mass spectrometer (UPLC-ESI-HRMS). The authors reported that SOA yield found to be about 7 times high in dry condition (RH_13%) than that in wet condition (RH_75%). Overall, the experimental data to show the impact of RH on SOA yields and products and the conclusion originating from the chamber are doubtful. The small chamber used in this study will be significantly influenced by the gas-wall processes of organic species increasing the uncertainty in data and interpretation of results. This paper in its current form is not acceptable. Please find the comments below.

The chamber volume for our current experiments was around 1 m^3. All chambers have the wall losses of species. Though a larger volume reactor may minimize these effects, the fans are usually equipped inside this kind of reactor to make the heat generated by lights homogeneously mixed, which counteracts the decrease of wall effect by the larger volume (Carter et al., 2005; Cocker et al., 2001). In addition, relatively small reactors in the range of 0.2-3 m^3 are also ubiquitously used in smog chamber studies (Chen et al., 2017; Chu et al., 2016; Díaz-de-Mera et al., 2017; Huang et al., 2017; Peng et al., 2017; Schnitzler et al., 2014; Ye et al., 2018). After careful analysis of our experiments, we believe that our results are reliable and credible. Below are the specific replies to the comments.

Carter, W., Cockeriii, D., Fitz, D., Malkina, I., Bumiller, K., Sauer, C., Pisano, J., Bufalino, C., and Song, C.: A new environmental chamber for evaluation of gas-phase chemical mechanisms and secondary aerosol formation, Atmos. Environ., 39, 7768-7788, 10.1016/j.atmosenv.2005.08.040, 2005.

Chen, L., Bao, K., Li, K., Lv, B., Bao, Z., Lin, C., Wu, X., Zheng, C., Gao, X., and Cen, K.: Ozone and secondary organic aerosol formation of toluene/NO_x irradiations under complex pollution scenarios, Aerosol Air Qual. Res., 17, 1760-1771, 10.4209/aaqr.2017.05.0179, 2017.

Chu, B., Zhang, X., Liu, Y., He, H., Sun, Y., Jiang, J., Li, J., and Hao, J.: Synergetic formation of secondary inorganic and organic aerosol: effect of SO_2 and NH_3 on particle formation and growth, Atmos. Chem. Phys., 16, 14219-14230, 10.5194/acp-16-14219-2016, 2016.

Cocker, D. R., 3rd, Flagan, R. C., and Seinfeld, J. H.: State-of-the-art chamber facility for studying atmospheric aerosol chemistry, Environ. Sci. Technol., 35, 2594-2601, 10.1021/es0019169, 2001.

Díaz-de-Mera, Y., Aranda, A., Martínez, E., Rodríguez, A. A., Rodríguez, D., and Rodríguez, A.: Formation of secondary aerosols from the ozonolysis of styrene: Effect of SO_2 and H_2O, Atmos. Environ., 171, 25-31, 10.1016/j.atmosenv.2017.10.011, 2017.

Huang, M., Hao, L., Cai, S., Gu, X., Zhang, W., Hu, C., Wang, Z., Fang, L., and Zhang, W.: Effects of inorganic seed aerosols on the particulate products of aged 1,3,5-trimethylbenzene secondary organic aerosol, Atmos. Environ., 152, 490-502, 10.1016/j.atmosenv.2017.01.010, 2017.

Peng, J., Hu, M., Du, Z., Wang, Y., Zheng, J., Zhang, W., Yang, Y., Qin, Y., Zheng, R., Xiao, Y., Wu, Y., Lu, S., Wu, Z., Guo, S., Mao, H., and Shuai, S.: Gasoline aromatics: a critical determinant of urban secondary organic aerosol formation, Atmos. Chem. Phys., 17, 10743-10752, 10.5194/acp-17-10743-2017, 2017.

Schnitzler, E. G., Dutt, A., Charbonneau, A. M., Olfert, J. S., and Jaeger, W.: Soot aggregate restructuring due to coatings of secondary organic aerosol derived from aromatic precursors, Environ. Sci. Technol., 48, 14309-14316, 10.1021/es503699b, 2014.

Ye, J., Abbatt, J. P. D., and Chan, A. W. H.: Novel pathway of SO_2 oxidation in the atmosphere: reactions with monoterpene ozonolysis intermediates and secondary organic aerosol, Atmos. Chem. Phys., 18, 5549-5565, 10.5194/acp-18-5549-2018, 2018.

Major Comments:

1. The aromatics VOCs are gas pollutants that is found to be high in urban environments where the NOx is also abundant. It is unclear why the authors chose no NOx condition to study the humidity effects on the formation of xylene SOA. Clarify this.

It is true that aromatics are found to be high in urban environments where NO_x is also abundant. Real environment is relatively complicated. Nevertheless, the purpose of our study is to investigate the RH effect on the SOA formation from *m*-xylene only oxidized by the OH radicals and not interpreted by other factors. The NO_x can complicate the aromatics oxidation system, since NO_x conditions can provide both OH and NO_3 radicals, and NO_x themselves can also participate in the oxidation reactions.

2. What is the effect of the wall on the loss gaseous H2O2? H2O2 is very hydrophilic and sticky to the wall. When RH is high, the water on the chamber wall becomes high forming a water film. This wet film can absorb a large amount of H2O2 and modulate the concentration of OH radicals. Please clarify how the authors measured OH radical concentrations under varying RH conditions. Why did the author use 20 ppm of H2O2 which was 40 times higher than the m-xylene concentration? What is the photolysis rate constant of H2O2 in the chamber?

We agree with the reviewer that H_2O_2 is very hydrophilic. According to the reviewer's comment, we estimated the wall loss of H_2O_2 at low and high RH at 299 K for 4 h in our study using the O_3 analyzer (49C, Thermo Environmental Instruments Inc.), since H_2O_2 can also absorb the light at 254 nm. Thus, the output by O_3 analyzer can basically represent the relative change in H_2O_2 concentration though it is not the real H_2O_2 concentration. The results for H_2O_2 wall loss experiments show that the numbers outputted by O_3 analyzer were in the range of 22.2-23.2 at low RH (8%) and in the range of 22.1-23.3 at high RH (75%) throughout each H_2O_2 wall loss experiment, respectively. Results indicate that there is no significant H_2O_2 wall loss throughout the experiments and no obvious difference between both RHs. In other words, H_2O_2 concentrations in the chamber were roughly constant during the experiment.

In this study there was no equipment for the measurement of OH radical concentrations, so we cannot directly obtain the OH radical concentration during the experiments. But it can be convinced that the OH concentrations were consistent at varying RHs, which can be realized from the similar change in concentrations of the reacted *m*-xylene (Fig. S1) (see below) that is added in the supplementary information according to the Comment 6 of the Reviewer 1. In addition, the MCM simulation was conducted to obtain the OH concentration of 1.6×10^{-4} ppb, for which a photolysis rate constant of 7.56×10^{-6} min^{-1} for H_2O_2 was used in the chamber.

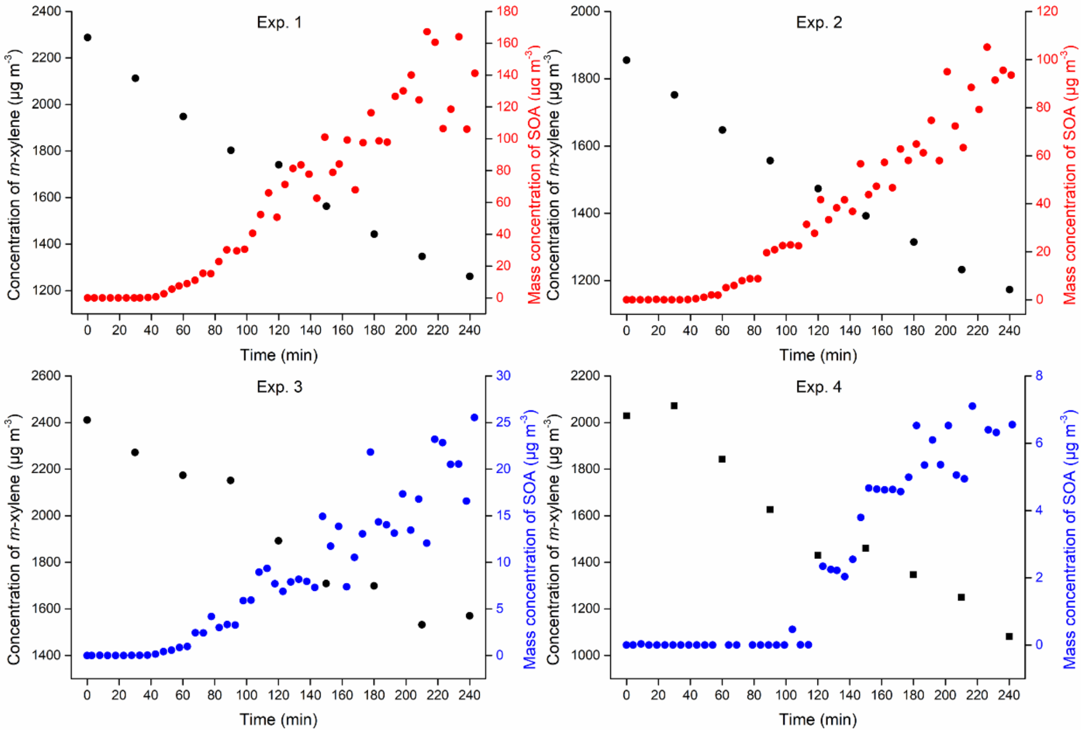

Fig. S1. Reaction time profiles of *m*-xylene measured by the GC-MS that accompanied the observed SOA growth for the four experiments

3. The size of chamber used in this study was one cubic meter and relatively very small. Thus, the wall of chemical species is very high. Additionally, the loss of chemical species to the chamber is very sensitive to humidity. The impact of RH on SOA yields can be very uncertain and doubtful. The reduction of SOA yields at the high humidity is more likely due to the chemical loss to the wet chamber wall. Thus, the conclusion made by the authors could be incorrect. Hydrophilic products and reactive chemical species can more deposit to the wall at high humidity.

We agree with the reviewer that the reactor volume in this study is relatively small. As we mentioned in the beginning of reply to Reviewer 2, in recent years small reactors in the range of (0.2-3) m^3 are ubiquitously used in smog chamber studies. Indeed, small chambers have the wall losses of species, but wall effects also exist in big reactors, since big reactor is needed to be equipped with fans inside the reactor to make the heat generated by lights homogeneously mixed. For small reactors, the particle wall loss of 5.87×10^{-5} s^{-1} was measured in a 3 m^3 reactor (Chen et al., 2017) and $(3.21\text{-}5.57) \times 10^{-5}$ s^{-1} was measured in a 2 m^3 reactor (Chu et al., 2016). For big reactors, the particle wall loss of 8×10^{-5} s^{-1} was measured in a 90 m^3 reactor (Carter et al., 2005) and $(2.5\text{-}5.0) \times 10^{-5}$ s^{-1} was measured in the dual 28 m^3 (Cocker et al., 2001). It is obvious that the particle wall loss from different researchers is different, but there is no clear relation between particle wall loss and reactor volume for the reactor volume of over 1 m^3. It can be speculated that wall effects for other chemical species are probably similar between small and big reactors.

In addition, we agree with the reviewer that the loss of chemical species to the wall is sensitive to humidity. To clarify this, we have added a paragraph at the end of Sec. 3.1 following the newly added paragraph according to the Comment 2 of Review 1 in the revised manuscript to clarify the possible underestimation of SOA mass and the reliability of our study.

The wall loss of chemical species that is sensitive to humidity may affect the RH effect on SOA yields, as the reduction of SOA yields at the high humidity may be due to the chemical loss to the wet chamber wall. To estimate the extent of how much the wall loss of chemical species affects the SOA formation at different RHs, we take glyoxal and acetone as reference compounds. Glyoxal, a typical compound that can form SOA, can easily dissolve in the aqueous phase due to the large Henry's law constant of 4.19×10^5 M atm^{-1} (Ip et al., 2009), very sensitive to humidity. Loza et al. (2010) found that the wall loss of glyoxal was minimal at 5% RH, with $k_W = 9.6 \times 10^{-7}$ s^{-1}, whereas k_W was 4.7×10^{-5} s^{-1} at 61% RH. We assume that k_W linearly increases with RH, and the k_W value is estimated to be 6.1×10^{-5} s^{-1} at 80% and 7.4×10^{-6} at 13% RH, with the difference being 8.2 times. According to the wall loss of glyoxal, glyoxal only decreased by 10% at the end of our experiment at low RH, while glyoxal decreased by 59% at high RH. Acetone can hardly dissolve in the aqueous phase due to the small Henry's law constant of 29 M atm^{-1} (Poulain et al., 2010), which is 4 orders of magnitude less than that of glyoxal. Ge et al. (2017) obtained that the wall loss of acetone was 5.0×10^{-6} s^{-1} at 87% RH and 3.3×10^{-6} s^{-1} at 5% RH, with a factor of 1.5. The difference of wall loss between glyoxal and acetone at low RH is about 2 times, while it becomes about 12 times at high RH. Thus, it can be considered that the wall loss among different species at low RH is less affected by the Henry's law constant, but it is greatly affected at high RH. In our study glycolaldehyde (See the Sec. 3.3) is found to be an important SOA precursor that can form a large fraction of oligomers in our experiments, but the wall loss of glycolaldehyde is not available. The Henry's law constant of glycolaldehyde was obtained to be 4.14×10^4 M atm^{-1} (Betterton and Hoffmann, 1988), an order of magnitude lower than glyoxal, indicating that glycolaldehyde is less sensitive to humidity than glyoxal but much more sensitive to humidity than acetone. Based on the data of these two reference species, the wall loss of glycolaldehyde at low RH is taken to be 5×10^{-6} s^{-1}, and the difference in wall loss between high and low RHs is about 6 times. Then, the wall loss of glycolaldehyde at high RH can be 3×10^{-5} s^{-1}. Then, it is estimated that glycolaldehyde would decrease by 7% at low RH and by 35% at high RH at the end of our experiment, respectively. This means that SOA yield would be underestimated by 35% at high RH and by 7% at low RH if glycolaldehyde lost to the wall was completely transformed to SOA. If this wall effect of SOA precursors was taken into consideration, the SOA yields at high (Exp. 3) and low (Exp. 2) RHs would be 3.4% and 15.1%, respectively. Alternatively, the SOA yield at high RH was underestimated to be 42% relative to that at low RH. Even the sensitivity of the wall loss to RH was taken to be 8 times, the SOA yield at high RH would be underestimated to be 62% compared to that at low RH. In fact, there were many different SOA precursors from the *m*-xylene oxidation system that probably have much smaller Henry's law constant relative to that of glycolaldehyde. Thus, it is concluded that the RH effect on SOA formation from *m*-xylene oxidation by H_2O_2 without NO_x is negative.

Betterton, E. A. and Hoffmann, M. R.: Henry's law constants of some environmentally important aldehydes, Environ. Sci. Technol., 12, 1415-1418, 10.1021/es00177a004, 1988.

Carter, W., Cockeriii, D., Fitz, D., Malkina, I., Bumiller, K., Sauer, C., Pisano, J., Bufalino, C., and Song, C.: A new environmental chamber for evaluation of gas-phase chemical mechanisms and secondary aerosol formation, Atmos. Environ., 39, 7768-7788, 10.1016/j.atmosenv.2005.08.040, 2005.

Chen, L., Bao, K., Li, K., Lv, B., Bao, Z., Lin, C., Wu, X., Zheng, C., Gao, X., and Cen, K.: Ozone and secondary organic aerosol formation of toluene/NO_x irradiations under complex pollution scenarios, Aerosol Air Qual. Res., 17, 1760-1771, 10.4209/aaqr.2017.05.0179, 2017.

Chu, B., Zhang, X., Liu, Y., He, H., Sun, Y., Jiang, J., Li, J., and Hao, J.: Synergetic formation of secondary inorganic and organic aerosol: effect of SO_2 and NH_3 on particle formation and growth, Atmos. Chem. Phys., 16, 14219-14230, 10.5194/acp-16-14219-2016, 2016.

Cocker, D. R., 3rd, Flagan, R. C., and Seinfeld, J. H.: State-of-the-art chamber facility for studying atmospheric aerosol chemistry, Environ. Sci. Technol., 35, 2594-2601, 10.1021/es0019169, 2001.

Ge, S., Xu, Y., and Jia, L.: Effects of inorganic seeds on secondary organic aerosol formation from photochemical oxidation of acetone in a chamber, Atmos. Environ., 170, 205-215, 10.1016/j.atmosenv.2017.09.036, 2017.

Ip, H. S. S., Huang, X. H. H., and Yu, J. Z.: Effective Henry's law constants of glyoxal, glyoxylic acid, and glycolic acid, Geophys. Res. Lett., 36, L01802, 10.1029/2008gl036212, 2009.

Loza, C. L., Chan, A. W., Galloway, M. M., Keutsch, F. N., Flagan, R. C., and Seinfeld, J. H.: Characterization of vapor wall loss in laboratory chambers, Environ. Sci. Technol., 13, 5074-5078, 10.1021/es100727v, 2010.

Poulain, L., Katrib, Y., Isikli, E., Liu, Y., Wortham, H., Mirabel, P., Le Calve, S., and Monod, A.: In-cloud multiphase behavior of acetone in the troposphere: gas uptake, Henry's law equilibrium and aqueous phase photooxidation, Chemosphere, 81, 312-320, 10.1016/j.chemosphere.2010.07.032, 2010.

4. In order to analyze the chemical compositions in gas and particles phase using a variety of aerosol, a large amount of air volume should be collected. The size of the chamber used in this study was only one cubic. It is hard to believe how the authors analyzed gas and aerosol with the air volume less than one cubic meter. Additionally, the chamber volume was getting small as the experiment progressed. The consumption of the chamber air increased the wall effect. The authors should clarify this problem.

It is true that the chamber volume was getting small as the experiment progressed, but the change was not significant. The measurement of *m*-xylene concentration was conducted once every 30 min by a one-liter summa canister, so the total sampling volume for *m*-xylene measurement was only 9 L throughout each experiment. We also monitored the concentrations of ozone and NO_x once an hour by sampling 5 min, so the total sampling volume for ozone and NO_x measurement was only 30 L. The SMPS was on-line analysis, for which the flow rate was 0.3 L min^{-1}, and thus the total sampling volume was 72 L. Thus, before the SOA sampling, when the reaction stopped, the total volume for sampling was only around 110 L, approximately 10% of the size of reactor. Thus, the wall effect for gases and particles would not be significantly changed. After the reaction was finished, the DLPI and PILS simultaneously sampled for FTIR and HRMS analysis of chemical compositions of SOA, respectively. The DLPI sampled 150 L and the PILS needed 100 L. Thus, after the experiment was completely finished, the reactor still contained more than 700 L of air.

5. Page 5, line 4. The Master Chemical Mechanism can only provide the gas-phase reaction pathways. The yield of the products in particle phase may not directly connected to the yield of products in gas-phase. How does the author compare gas-phase oxygenated m-xylene products predicted using MCM to the measured particle-phase products from HRMS?

We agree with the reviewer that the MCM only provides the gas-phase reaction pathways. We went through the products in the MCM, and put the structure of these products in the Mass Frontier program, which can simulate the breakage of bonds made by the MS/MS analysis of HRMS. Meanwhile, we found 5 products in the gas phase by MCM those can match the HRMS analysis. These 5 products are considered to likely partition into the particle phase from the gas phase. Though we only find 5 products in the particle phase identified by HRMS that are also predicted in the gas phase by MCM, the MCM prediction can provide the formation pathway of RO_2 radicals, which are helpful with the prediction of RO_2 autoxidation.

6. Page 5, line 11. The value of the maximum SOA mass in Figure 1 is not consist with the values reported in the text and the Table 1. The value of SOA mass under 73.6% and 79.1% in Figure 1 is about 40 and 10 ug/m3 but the value reported in the text is only 1.9 and 0.8 ug/m3 and the value reported in Table 1 is 15.8 and 7.9 ug/m3.

There are indeed some mistakes in the text and in Fig. 1. Together with the reply to the Comment 3 of Reviewer 1, the SOA mass was re-corrected by the particle wall loss rates. The values of the maximum SOA mass under 73.6% and 79.1% RH are 21.0 and 7.5 ug/m^3, respectively. We have modified in Page 5, line 11 in the text and in Fig 1. A sentence has been added in the revised manuscript: "The maximum mass concentrations fitted are 150.3 and 95.5 μg m^{-3} at low RHs, whereas they are 21.0 and 7.5 μg m^{-3} at high RHs, …"

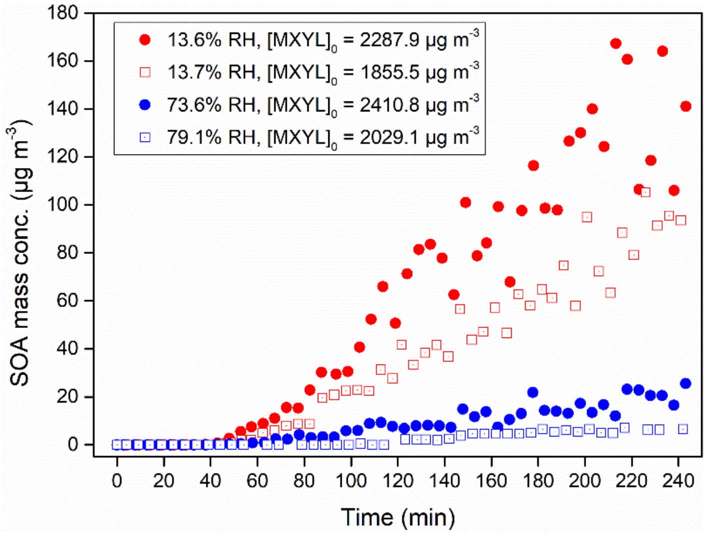

Figure 1. SOA mass concentrations as a function of irradiation time (corrected by particle wall loss and subtracted by LWC).

7 It is not clear how much LWC was present at the end of experiments and how much SOA mass was obtained after subtracting the LWC from total aerosol mass. What is the effects of LWC on the SOA formation in this study? The author mention that LWC can explain the positive effect of RH on SOA formation under high NOx condition. What is the difference in LWC between SOA with the high NOx condition and that with the low or no NOx condition?

At the end of experiments LWC volume concentration accounts for 34% and 45% in the Exps. 3-4 of the volume concentrations of wet particles, which are 5.1 and 2.4 μg m^{-3}, respectively. SOA mass obtained after subtracting the LWC from total aerosol mass were 21.0 and 7.5 μg/m^3 under 73.6% and 79.1% RH, respectively. The LWC has a negative effect on SOA formation in our study. LWC can generally promote SOA formation under high NO$_x$ condition, which was reported in many previous studies (Healy et al., 2009; Kamens et al., 2011; Zhou et al., 2011; Jia and Xu, 2014, 2018; Wang et al., 2016), but the recent study by Hinks et al. (2018) indicates the negative effect of RH on SOA. Although we did not conduct any experiments of *m*-xylene under high NO$_x$ condition, in previous studies, the LWC volume concentration was found to be 22% (78% RH, Jia and Xu, 2018) and 17% (85% RH, Prenni et al., 2007) of wet SOA volume concentration from toluene photoxidation under NO$_x$ concentrations of 300 ppb. This indicates that LWC is larger under the high NO$_x$ condition than under the low or no NO$_x$ condition.

Healy, R. M., Temime, B., Kuprovskyte, K., and Wenger, J. C.: Effect of relative humidity on gas/particle partitioning and aerosol mass yield in the photooxidation of *p*-xylene, Environ. Sci. Technol., 43, 1884-1889, 10.1021/es802404z, 2009.

Hinks, M. L., Montoya-Aguilera, J., Ellison, L., Lin, P., Laskin, A., Laskin, J., Shiraiwa, M., Dabdub, D., and Nizkorodov, S. A.: Effect of relative humidity on the composition of secondary organic aerosol from the oxidation of toluene, Atmos. Chem.

Phys., 18, 1643-1652, 10.5194/acp-18-1643-2018, 2018.

Jia, L., and Xu, Y.: Effects of relative humidity on ozone and secondary organic aerosol formation from the photooxidation of benzene and ethylbenzene, Aerosol Sci. Technol., 48, 1-12, 10.1080/02786826.2013.847269, 2014.

Jia, L., and Xu, Y.: Different roles of water in secondary organic aerosol formation from toluene and isoprene, Atmos. Chem. Phys., 18, 8137-8154, 10.5194/acp-18-8137-2018, 2018.

Kamens, R. M., Zhang, H., Chen, E. H., Zhou, Y., Parikh, H. M., Wilson, R. L., Galloway, K. E., and Rosen, E. P.: Secondary organic aerosol formation from toluene in an atmospheric hydrocarbon mixture: Water and particle seed effects, Atmos. Environ., 45, 2324-2334, 10.1016/j.atmosenv.2010.11.007, 2011.

Prenni, A. J., Petters, M. D., Kreidenweis, S. M., DeMott, P. J., and Ziemann, P. J.: Cloud droplet activation of secondary organic aerosol, J. Geophys. Res., 112, D10223, 10.1029/2006JD007963, 2007.

Wang, Y., Luo, H., Jia, L., and Ge, S.: Effect of particle water on ozone and secondary organic aerosol formation from benzene-NO_2-NaCl irradiations, Atmos. Environ., 140, 386-394, 10.1016/j.atmosenv.2016.06.022, 2016.

Zhou, Y., Zhang, H., Parikh, H. M., Chen, E. H., Rattanavaraha, W., Rosen, E. P., Wang, W., and Kamens, R. M.: Secondary organic aerosol formation from xylenes and mixtures of toluene and xylenes in an atmospheric urban hydrocarbon mixture: Water and particle seed effects (II), Atmos. Environ., 45, 3882-3890, 10.1016/j.atmosenv.2010.12.048, 2011.

8. What is the particle size distribution of m-xylene SOA? Does all of the particle size smaller than 1000 nm and within the SMPS measurement range?

According to the reviewer's comment, we have added the particle size distribution of *m*-xylene SOA for the four experiments in the supplementary information (see Fig. S2). As shown in Fig. S2, all of the particle size is smaller than 1000 nm and within the SMPS measurement range.

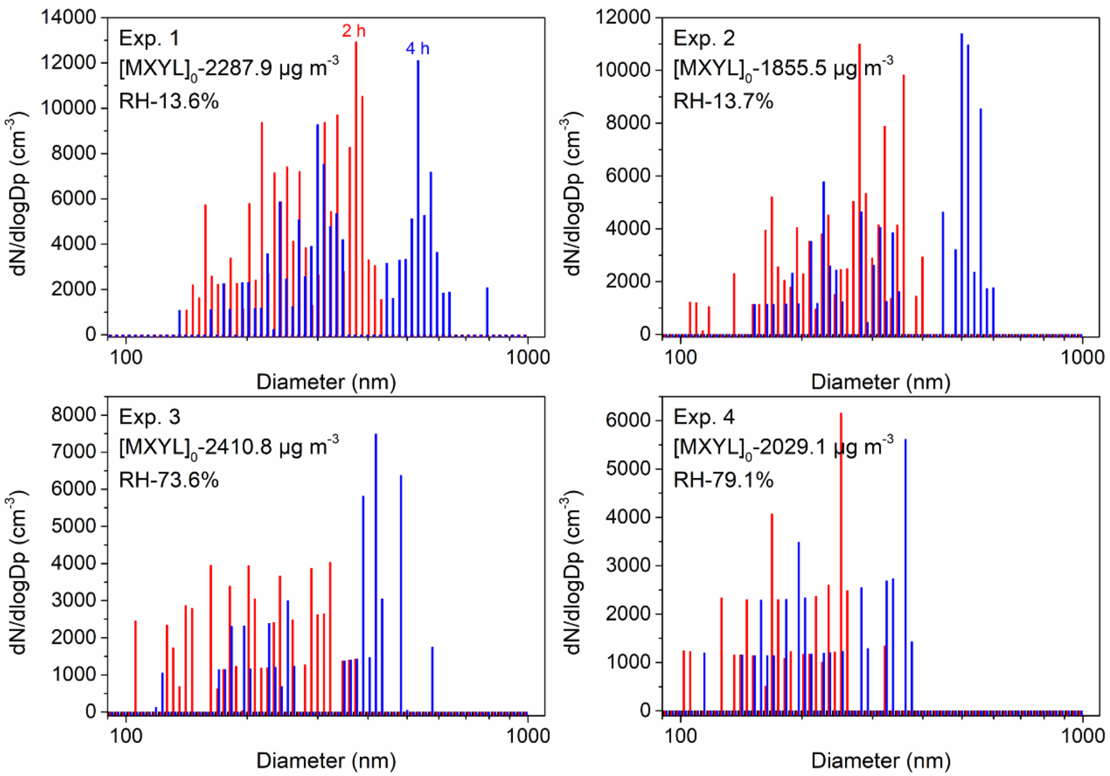

Fig. S2 Variations of particle size distribution of number and mass concentrations at the 2-h time point and at the end of the experiment for the four experiments.

9. Section 3.2. The intensity of the functional groups in FTIR spectrum was correlated to the sample mass. What was the SOA mass that collected on the disk and that measured using FTIR? Or does the author use same sampling duration for both RH conditions? What was the collection efficiency of the impactor on a sampling disk as a function of the particle size? Without knowing the mass of measured SOA, it is unreasonable to compare the peak intensity of the functional group between SOA from different samples.

We did not measure the mass of SOA collected on the disk, as the weight of ZnSe window is several grams, much larger than the SOA mass that is only several micrograms. We used the same sampling duration for both RH conditions and the FTIR spectra under different RH conditions can be comparable. The DLPI sampling flow rate was 10 L min^{-1}, and the sampling duration was 15 min. The total collection efficiency of the DLPI was 87%, and the efficiency varies for different impaction stages (Durand et al., 2014). DLPI has 13 stages. When we sampled using DLPI, the four plates for stages 4-7 were removed, so that particles in the range of 108-650 nm were collected on the third plate. As shown in Fig. S2 that is newly added in the reply to Comment 8, the particles in the range of 108-650 nm can represent the total SOA from *m*-xylene oxidation in this study. The mean collection efficiency of the DLPI for stages 4-7 is around 83% (Durand et al., 2014). SOA mass was obtained by the calculation based on the SMPS measurement and the DLPI collection efficiency, 10.3 and 3.0 μg at low RH (Exp. 2) and high RH (Exp. 3). The ratio of the SOA mass collected on disk at high RH to that at low RH is 0.29. The relative intensities of most functional groups in Table 2 match this SOA mass ratio. According to the reviewer's comment, we have added some sentences about the SOA mass collected on the ZnSe window after the first sentence of Sec. 3.2.

The DLPI sample flow rate was 10 L min^{-1}, and the sampling duration was 15 min. We used same sampling flow rate and duration for both RH conditions. DLPI has 13 stages, and it can collect particles in the size range of 30 nm - 10 mm. When we sampled using DLPI, the four plates for stages 4-7 were removed, so that particles in the range of 108-650 nm were collected on the third plate. As shown in Fig. S2 in the supplementary information, the particles in the range of 108-650 nm can represent the total SOA from *m*-xylene oxidation in this study. The mean collection efficiency of the DLPI was 83% for stages 4-7 (Durand et al., 2014). Thus, the SOA mass collected on the ZnSe window was 10.3 and 3.0 μg at low RH (Exp. 2) and high RH (Exp. 3), based on the SMPS measurement and the DLPI collection efficiency.

Durand, T., Bau, S., Morele, Y., Matera, V., Bémer, D., and Rousset, D.: Quantification of low pressure impactor wall deposits during zinc nanoparticle sampling, Aerosol Air Qual. Res., 14, 1812-1821, 10.4209/aaqr.2013.10.0304, 2014.

10. Figure 2 and Table 2. There is also peak at 3000 cm-1 which is missing in Table 2.

Taking the reviewer's suggestion, we have added the peak at 3000 cm^{-1} in Table 2.

Table 2. Absorbance positions of functional groups and the intensities at low and high RHs.

Absorption frequencies	Functionality	Intensity (× 10^{-3})		Ratio [a]
		low RH	high RH	
3235	O-H	5.9	1.9	0.32
3000	C-H	4.5	1.4	0.31
1720	C=O	5.1	1.5	0.29
1415	CO-H	4.8	2.4	0.50
1180	C-O-C, C-O and OH of COOH	2.9	1.4	0.48
1080	C-C-OH	5.3	1.8	0.34

[a] Ratio of the intensity at high RH to that at low RH.

11. What is the measured glyoxal fraction in m-xylene SOA? Was oligomerization impacted by the RH in this study? Even though the concentration of highly oxygenated molecule (HOM) is much lower at high RH, the overall trend of the SOA mass, which is much less at high RH compare to low RH, cannot be explained by solely through HOMs. As mentioned in the previous comment above, the effect of the wet wall on SOA formation can be very significant particularly in small reaction. The time scale of the gas-wall partitioning of organic species can be significantly fast and results in the less SOA yields at higher humidity.

Glyoxal in SOA was not observed in our study. Instead, we obtained the glycolaldehyde ($C_2H_4O_2$) fraction in SOA from MS/MS analysis which has been observed previously in the oxidation of *m*-xylene (Cocker et al., 2001). The RH suppresses oligomerization in this study as can be obviously observed in Fig. 4. In oligomerization reaction of glycolaldehyde with carbonyls by aldol condensation reactions, water is involved as a by-product, leading to the suppression of the oligomerization by high RH.
Indeed, we agree with the reviewer that it cannot be solely explained through HOMs that SOA mass at high RH is much less than that at low RH. To further explain the large discrepancy of SOA mass at low and high RHs, we have added a paragraph at the end of the Sec. 3.4.

The wall process of the reactor enlarges the difference of SOA mass between low and high RH. The wall loss of some chemical species is faster at high RH, which leads to the reduction of SOA yield. In addition, the difference of SOA mass can be also enhanced based on the gas to particle partitioning rule (Li et al, 2018).

Li, K., Li, J., Wang, W., Li, J., Peng, C., Wang, D., and Ge, M.: Effects of gas-particle partitioning on refractive index and chemical composition of *m*-xylene secondary organic aerosol, J. Phys. Chem. A, 122, 3250-3260, 10.1021/acs.jpca.7b12792, 2018.

12 The author claimed that the increase of the C-O-C stretching was resulted from the oligomerization of carbonyls under the high RH condition. However, the IR absorption at 1080 cm-1 can be also due to the existence of C-OH group. Clarify this.

The statement in the text was incorrect. The relative intensity of the C-O-C group is higher than that of the C=O group, indicating that C-O-C group is more than other functional groups at high RH, which does not mean that the oligomerization is higher at high RH. We have deleted the corresponding sentence in the last second sentence of the Sec. 3.2.

13. Fig. 2. Authors assigned the peak at 1600 cm-1 as carboxylate. The reviewer doubt this assignment. In general, dry organic aerosol cannot produce carboxylic acid ions. Even if the organic aerosol is produce in the wet condition, the aerosol

water content is not enough to product the dissociation of carboxylic acid. In general, the pKa of carboxylic acid ranges from 2 to 6. Even in the dilution in water, less than 1% of carboxylic acid is dissociable. In SOA, most carboxylic acids will be in the un-dissociated form.

We agree with the reviewer's comment that the peak in 1605 cm^{-1} cannot be assigned to dissociation of carboxylic acid. Thus, we have deleted the peak assignment in Table 2 and deleted the corresponding sentence in the second and third paragraph of the Sec. 3.2.

Table 2. Absorbance positions of functional groups and the intensities at low and high RHs.

Absorption frequencies	Functionality	Intensity ($\times 10^{-3}$)		Ratio [a]
		low RH	high RH	
3235	O-H	5.9	1.9	0.32
3000	C-H	4.5	1.4	0.31
1720	C=O	5.1	1.5	0.29
1415	CO-H	4.8	2.4	0.50
1180	C-O-C, C-O and OH of COOH	2.9	1.4	0.48
1080	C-C-OH	5.3	1.8	0.34

[a] Ratio of the intensity at high RH to that at low RH.

14. Fig. 4. Based on Fig. 4, a large mass appeared in negative ion mode suggesting that the aerosol has a large fraction of carboxylic acid. It is contradictable compared to either MCM simulation or the conclusion by the authors in the glyoxal was abundant. In general, a large fraction of gaseous products from MCM prediction are alcohols and carbonyls, and amount of carboxylic acids are small. Please clarify this.

Indeed, a large fraction of gaseous products from MCM prediction are alcohols and carbonyls and a few compounds are organic acids. Glyoxal is one of the relatively abundant gas-phase products in MCM simulation (about 20 ppb at the end of 4 h experiment). Carbonyls in SOA account for a large fraction of compounds that have been identified by HRMS in the positive mode (Fig. 4), some of which are in agreement with those in the gas phase simulated by MCM. In addition, we think that the large number of carboxylic acids observed in HRMS are also produced from the oxidation of organic species in the particle phase. In our original manuscript about FTIR analysis, we mentioned that the peak at 1080 cm-1 was assigned to be the C-C-OH, which could be considered as the glyoxal hydrate. This description may not be very accurate, since FTIR has limitation in identification of compounds. In further identification, the glyoxal fragment was not identified in HRMS analysis. For clarification of description of glyoxal in the text, some sentences started in Page 7 Line 7 have been modified.

The ratios of O-H, C-H, C=O and C-C-OH groups are 0.29 to 0.34, which is close to the ratio of SOA mass at high RH to that at low RH collected on the ZnSe disk, whereas the ratios of CO-H, C-O-C, C-O-H in COOH are above 0.48. The relative intensity of the C-O-C group is significantly higher than the C=O group, which can be explained by more oligomerization with the formation of C-O-C than other reactions at high RH. Nevertheless, the FTIR results cannot provide further information to well explain the differences of SOA yields between low and high RH, which will be further discussed in terms of mass spectra of SOA in the next section.

15. Fig. 4. Low carbon number products are generally more volatile than high carbon number products. Fig.4 showed that low carbon number products are high with the SOA with the low RH, possibly suggesting that volatile low carbon number products more likely deposited to the wall due to the gas-wall process.

Indeed, a fraction of low carbon number products at high RH are likely deposited to the wall. As we discussed in the reply to Comment 3, wall loss effects of organic vapors likely reduce formation of SOA, which is more obvious at high RH. However, it is considered that the decrease of low carbon number products in SOA are mainly due to the chemical reaction process at high RH.

16. What was the RH of the environment inside the FTIR spectrometer when FTIR spectra were obtained for Fig. 4?

The sample compartment of the FTIR spectrometer was purged by dry air desiccated from FTIR purge gas generator (Model 75-45-12VDC, Balston, Parker) ahead of the FTIR measurement. The dew point temperature of the dry gas from this generator is as low as -65 °C. So the RH of the environment inside the FTIR spectrometer was extremely low, close to zero when FTIR spectra were obtained for Fig. 4.

17. What is the atmospheric implication of this study? What is the potential impact of RH on p-xylene and o-xylene as well as other aromatics? Will other aromatics also have the similar RH effects with m-xylene? What is the uncertainty of this study? Does the impaction or the PILS sampling has uncertainty? What is the duration of the experiments?

The atmospheric implication of this study is that the production of SOA from aromatics in low-NO_x environments can be strongly modulated by the ambient RH probably due to the influence of H_2O on the formation of HOMs and oligomers. We proposed that the clear pathway of the influence of H_2O on the formation of HOMs needs to be further studied in the future. Negative RH effect on the SOA yield is a common feature of the monocyclic aromatics oxidation under low NO_x conditions and using H_2O_2 as the OH radical source from the previous study on toluene SOA and this study on *m*-xylene SOA. The uncertainty of this study is mainly from the wall loss of chemical species at different RHs. In a previous study (Sorooshian et al., 2006), the PILS sampling uncertainty was reported to be 6%. The uncertainty of DLPI sampling was around 20%

(Durand et al., 2014). The duration of the experiments was 4 h. Based on the reviewer's comment, we have added a sentence at the end of the Sec. 2.1 "The experiments were conducted for 4 h." and we have modified the Sec. 4 for clarification of the atmospheric implication.

Durand, T., Bau, S., Morele, Y., Matera, V., Bémer, D., and Rousset, D.: Quantification of low pressure impactor wall deposits during zinc nanoparticle sampling, Aerosol Air Qual. Res., 14, 1812-1821, 10.4209/aaqr.2013.10.0304, 2014.

Sorooshian, A., Brechtel, F. J., Ma, Y., Weber, R. J., Corless, A., Flagan, R. C., Seinfeld, J. H.: Modeling and characterization of a particle-into-liquid sampler (PILS), Aerosol Sci. Technol., 40, 396-409, 10.1080/02786820600632282, 2006.

The current study investigates the effect of RH on SOA formation from the oxidation of *m*-xylene under low NO_x conditions in the absence of seed particles. The elevated RH can significantly obstruct the SOA formation from the *m*-xylene-OH system, so that the SOA yield decrease from 13.8% at low RH to 0.8% at high RH, with a significant discrepancy of higher than one order of magnitude. The FTIR results of functional groups show the relative increase of the C-O-C group at high RH as compared with low RH, indicating that the oligomers from carbonyl compounds cannot well explain the suppression of SOA yield. HOMs were observed to be suppressed in the HRMS spectra. The chemical mechanism for explaining the obvious difference of RH effects on SOA formation from *m*-xylene-OH system has been proposed based on the analysis of both FTIR and HRMS measurements as well as MCM simulations. The reduced SOA at high RH is mainly ascribed to the less formation of oligomers and the suppression of RO_2 autoxidation. Together with the previous study on toluene SOA, it is conceivable that the negative RH effect on the SOA yield is a common feature of the monocyclic aromatics oxidation under low NOx conditions and using H_2O_2 as the OH radical source. Our results obviously indicate that the production of SOA from aromatics in low-NO_x environments can be strongly modulated by the ambient RH probably due to the influence of H_2O on the formation of HOMs and oligomers. Our study highlights the role of water in the SOA formation, which is particularly related to chemical mechanisms used to explain observed air quality and to predict chemistry in air quality models and climate models. The clear pathway of the influence of H_2O on the formation of HOMs needs to be further studied in the future.

18. There are numerous grammatical problems. The manuscript needs to be approved by a native English speaker.

According to the advice of the reviewer, we have read the manuscript carefully and modified some sentences to correct grammatical errors.

19. Page 3 Line 13. The author may need to provide the reason why the author set the density of m-xylene SOA is set as 1.4 g/cm. According to the citation Ng et al. 2007 gives the density of m-xylene SOA as 1.33 _ 0.1 g/cm and Sato et al. 2007 provide the density of Toluene SOA as 1.42 _ 0.8 g/cm.

We agree with the reviewer's comment that the density we cited is not consistent with this study. We made a mistake when we cited references. Thus, we have corrected this mistake in the text, "To obtain the particle mass concentrations and SOA yield, an SOA density of 1.4 g cm^{-3} was used (Song et al., 2007)."

Song, C., Na, K., Warren, B., Malloy, Q., and Cocker, D. R., III: Secondary organic aerosol formation from *m*-xylene in the absence of NO_x, Environ. Sci. Technol., 41, 7409-7416, 10.1021/es070429r, 2007.

20. Page 3 Line 17. The author mention about the uncertainty of SMPS. However, the uncertainty of SMPS measurement for the used data in the paper was not reported.

As we mentioned in the text, SMPS measurement uncertainty is mainly dominated by size-dependent aerosol charging efficiency uncertainties and CPC sampling flow rate variability. The size-dependent aerosol charging efficiency is typically characterized by an accuracy of ± 10% (Jiang et al., 2014), which was used in our study to calculate the uncertainties of SOA mass concentration on the premise that the uncertainty of organic vapor wall loss was not included. The standard error of linear regression of the *m*-xylene concentration and peak area obtained by GC-MS was 0.013, which was extremely low compared with the *m*-xylene concentration and can be negligible. Thus, the uncertainty of 10% was used in SOA yield. In the revised manuscript, we have modified the Table 1 with the addition of uncertainty of SOA mass concentration.

Table 1. Experimental conditions, SOA concentrations and yields at the end of the experiments in *m*-xylene-OH oxidation system.

Exp. No.	[*m*-xylene]$_0$ (μg m^{-3})	[*m*-xylene]$_{reacted}$ (μg m^{-3})	RH (%)	T (°C)	[SOA]$_e$ (μg m^{-3})	SOA yield (%)
1	2287.9	1026.3	13.6	25.9	150.3 ± 15.0	14.6 ± 1.5
2	1855.5	682.0	13.7	25.3	95.5 ± 9.5	14.0 ± 1.4
3	2410.8	941.4	73.6	27.5	21.0 ± 2.1	2.2 ± 0.2
4	2029.1	946.9	79.1	27.4	7.5 ± 0.7	0.8 ± 0.1

[SOA]$_e$ indicates the mass concentration of SOA at the end of each experiment with particle wall loss corrected.

21. Page 4 Line 6. For comparing the SOA yield between cited values and that of this study, it may need to provide the error range of the values. Additionally, numerous data of this paper need errors.

We used the uncertainty of 10% to calculate SOA mass concentration from SMPS measurement. As we explained in Comment 21, the uncertainty of 10% was used in SOA yield (see Table 1 above).

22. Pages 6 and 7 (section 3.2): The description to construct the functional group distribution using FTIR spectra is unclear. How to separate the FTIR peaks for each functional group? The intensity of each function group varies with vibration force constant and peak broadening changes with compositions.

We used the peak height to represent the functional group distribution. The separation of FTIR peaks for each functional group was conducted by the peak valleys between two peaks.

Minor comments:

Page 2, line 21. The sentence is confused that it compares the RH effects between low NOx condition and with NOx condition.

Taking the reviewer's suggestion, we have corrected the sentence.

However, under low NOx level, it has been found that, in the study on toluene SOA formation, moderate RH level (48%) leads to a lower SOA yield than low RH level (17-18%).

Figure 3. The y-axis scale is negative for high RH and positive for Low RH. It is better to make them as a same positive scale.

Taking the reviewer's advice, we have modified the y-axis scale for high RH in Fig 3.

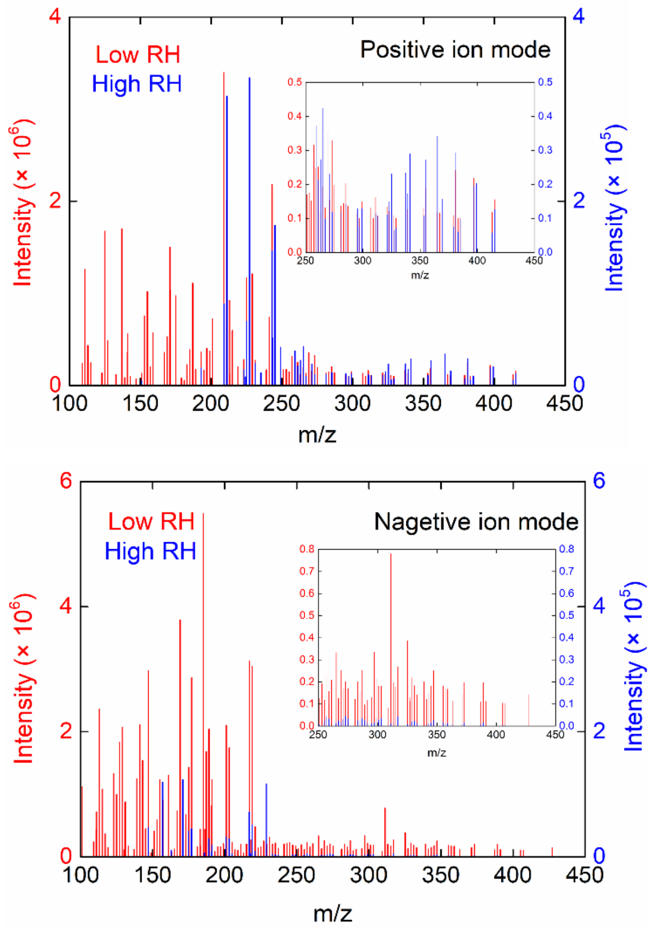

Figure 3. Selected background-subtraction HESI-Q Exactive-Orbitrap MS results of SOA in both positive and negative ion modes from the photooxidation of *m*-xylene-OH under both low and high RH conditions (Note that the Y-axis scales for low and high RH are largely different, 10^6 at low RH and 10^5 at high RH).

Figure 5: RH scale should range from 0 to 100 (negative is incorrect).

Taking the reviewer’s advice, we have modified the RH scale and corrected the negative scale in Fig 5.

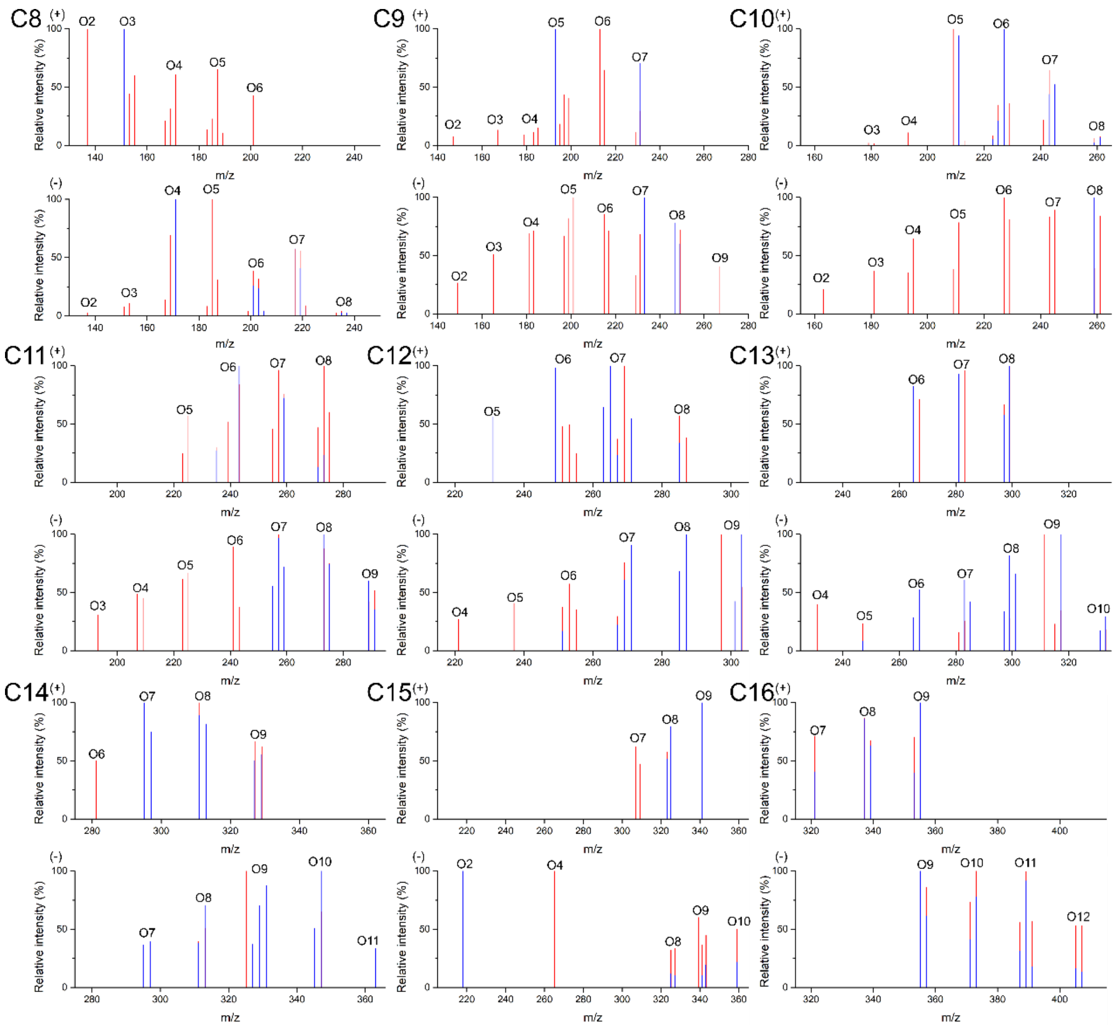

Figure 5. Mass spectra of SOA from *m*-xylene at both low (red) and high (blue) RH in the positive (+) and negative (-) ion modes, grouped with the same number of carbon atoms (from nC =8 to 16). On (n = 2, 3, ……, 12) means the number of oxygen atoms in the formula of the peak.

Page 2 line 15: it is better to use “have been conducted”.

Taking the reviewer’s advice, we have corrected this mistake, “Investigations of RH effects on aromatics SOA have been conducted in many previous works.”

Page 2 line 19: after “as an OH radical source,” there supposed to use period instead of comma.

In this sentence, "no NOx were introduced artificially and photolysis of H2O2 was as an OH radical source" is an appositive clause to explain the "condition", so the part before the comma is an adverbial modifier and thus we use a comma.

Table 3. The form of the table is better to unify with other tables.

Taking the reviewer's advice, we have unified the Table 3 with other tables.

Table 3. Plausibility of different types of compounds with elemental formulae measured by HRMS in the positive ion mode.

Low RH			High RH				
Measured (m/z)	Intensity	Error (mDa)	Measured (m/z)	Intensity	Error (mDa)	Ion formula	Proposed structure
137.0596	1.7×10^6	0.6	137.0593	1.4×10^5	1	$[C_8H_9O_2]^+$	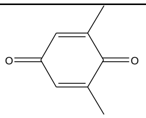
141.0545	5.6×10^6	1.3	141.0542	-	1.5	$[C_7H_9O_3]^+$	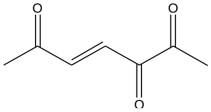
155.0701	1.0×10^6	1.2	155.0699	-	1.5	$[C_8H_{11}O_3]^+$	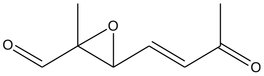
171.0651	1.0×10^6	1.2	171.0649	-	1.4	$[C_8H_{11}O_4]^+$	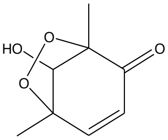
187.06	1.1×10^6	1.2	187.0568	-	4.4	$[C_8H_{11}O_5]^+$	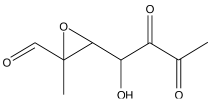

Secondary organic aerosol formation from OH-initiated oxidation of *m*-xylene: effects of relative humidity on yield and chemical composition

Qun Zhang[1,2], Yongfu Xu[1,2,*], Long Jia[1,2]

[1]State Key Laboratory of Atmospheric Boundary Layer Physics and Atmospheric Chemistry, Institute of Atmospheric Physics, Chinese Academy of Sciences, Beijing 100029, China,
[2]Department of Atmospheric Chemistry and Environmental Sciences, College of Earth Sciences, University of Chinese Academy of Sciences, Beijing 100049, China

Correspondence to: Yongfu Xu (xyf@mail.iap.ac.cn)

Abstract. The effect of relative humidity (RH) on the secondary organic aerosol (SOA) formation from the photooxidation of *m*-xylene initiated by OH radicals in the absence of seed particles was investigated in a smog chamber. The SOA yields were determined based on the particle mass concentrations measured with a scanning mobility particle sizer (SMPS) and reacted *m*-xylene concentrations measured with a gas chromatograph-mass spectrometer (GC-MS). The SOA components were analysed using Fourier transform infrared spectrometer (FTIR) and ultrahigh performance liquid chromatograph-electrospray ionization-high-resolution mass spectrometer (UPLC-ESI-HRMS). A significant discrepancy was observed in SOA mass concentration and yield variation with the RH conditions. The SOA yield is 13.8% and 0.8% at low RH (13.7%) and high RH (79.1%), respectively, with the difference being over an order of magnitude. The relative increase of C-O-C at high RH from the FTIR analysis of functional groups indicates that the oligomers from carbonyl compounds cannot well explain the suppression of SOA yield. Highly oxygenated molecules (HOMs) were observed to be suppressed in the HRMS spectra. The chemical mechanism for explaining the RH effects on SOA formation from *m*-xylene-OH system is proposed based on the analysis of both FTIR and HRMS measurements as well as Master Chemical Mechanism (MCM) simulations. The reduced SOA at high RH is mainly ascribed to the less formation of oligomers and the suppression of RO_2 autoxidation. As a result, high RH can obstruct the oligomerization and autoxidation that contribute to the SOA formation.

1 Introduction

Secondary organic aerosol (SOA) is a significant component of atmospheric fine particulate matter in the troposphere (Hallquist et al., 2009; Spracklen et al., 2011; Huang et al., 2014), leading to serious concerns as it has a significant influence on the air quality, oxidative capacity of the troposphere, global climate change and human health (Jacobson et al., 2000; Hansen and Sato, 2001; Kanakidou et al., 2005; Zhang et al., 2014). In a previous study from a global model simulation, it has been found that SOA represents a large fraction, approximately 80% of the total organic aerosol sources (Spracklen et al., 2011).

The formation of SOA in the atmosphere is principally via the oxidation of volatile organic compounds (VOCs) by common atmospheric oxidants such as O_3, OH and NO_3 radicals (Seinfeld and Pandis, 2016). Aromatic compounds mainly from anthropogenic source, including solvent usage, oil-fired vehicles and industrial emissions, contribute 20-30% to the total VOCs in urban atmosphere, which play a significant role in the formation of ozone and SOA in the urban troposphere (Forstner et al., 1997; Odum et al., 1997; Calvert et al., 2002; Bloss et al., 2005; Offenberg et al., 2007; Ding et al., 2012; Zhao et al., 2017). Amongst aromatics, *m*-xylene is significant, of which mean concentration together with *p*-xylene in daytime was determined up to 140.8 μg m^{-3} in atmosphere of urban areas in developing countries (Khoder, 2007).

The oxidation of aromatics in the troposphere is mainly initiated through OH radicals, which is affected by many chemical and physical factors. The concentrations of oxidant species, VOCs and NO_x concentrations, as well as the ratio of VOCs to NO_x (Ge et al., 2017a) determine the main chemical mechanism. Light intensity (Warren et al., 2008), temperature (Qi et al., 2010) and relative humidity (RH) are the most significant physical parameters that affect the chemical process. RH governs the water concentration in the gas phase and the liquid water content (LWC) in the particle phase. Water plays a significant role that can serve as reactant, product and solvent to directly participate in chemistry (Finlayson-Pitts and Pitts Jr., 2000) and indirectly affect the reaction environment such as acidity of particles (Jang et al., 2002).

Investigations of RH effects on aromatics SOA have been conducted in many previous works. In the presence of NO_x, it was observed that RH significantly enhanced the yield of SOA from benzene, toluene, ethylbenzene and xylenes photooxidation, which was explained by a higher formation of HONO, particle water, aqueous radical reactions and the hydration from glyoxal (Healy et al., 2009; Kamens et al., 2011; Zhou et al., 2011; Jia and Xu, 2014, 2018; Wang et al., 2016). Meanwhile, under low NO_x condition that no NO_x were introduced artificially and photolysis of H_2O_2 was as an OH radical source, it has been observed that deliquesced seed contributed to the enhancement of SOA yield from toluene (Faust et al., 2017; Liu et al., 2018). However, under low NO_x level, it has been found that, in the study on toluene SOA formation, moderate RH level (48%) leads to a lower SOA yield than low RH level (17-18%) (Cao and Jang, 2010). In a most recent study on SOA formation of toluene (Hinks et al., 2018), high RH led to a much lower SOA yield than low RH under low NO_x level, which is attributed to condensation reactions that remove water, leading to the less oligomerization at high RH. In a study on chemical oxidative potential of SOA (Tuet et al., 2017) under low NO_x conditions, it was observed that the mass concentration of SOA from *m*-xylene irradiation under the dry condition was much larger than that under the humid condition, whereas the study did not focus on the RH effect on *m*-xylene SOA formation. These demonstrate that the RH effects on aromatics SOA yields, especially *m*-xylene, have not been fully understood and the RH effects are controversial under various NO_x levels and seed particle conditions.

Chemical components of SOA are important, on which climate- and health-relevant properties of particles are dependent. Chemical compositions of SOA from aromatics-NO_x photooxidation have been investigated by GC/MS analysis (Forstner et al., 1997). Nevertheless, this study was only performed at 15-25% RH and high temperature at GC injection ports can easily decompose some low-volatile substances in SOA. FTIR was also used to study chemical compositions of SOA from aromatics-NO_x photooxidation under different RH conditions, in which the information of functional groups in SOA was provided (Jia and Xu, 2014, 2018). The recent study on SOA components from toluene-OH system under both dry and humid conditions were analysed via HRMS (Hinks et al., 2018). Although the information of chemical compositions in SOA has been given, the analysis and the mechanism of RH effects still need to be further studied.

The reaction of *m*-xylene-OH system forms peroxy radicals (RO_2) that can rapidly react with HO_2 to form RO (R2a) and ROOH (R2b). RO finally forms carbonylic products, such as (methyl) glyoxal and other SOA precursors (Jenkin et al., 2003; Hallquist et al., 2009; Carlton et al., 2010; Carter and Heo, 2013). In most recent studies, RO_2 autoxidation has been observed that leads to the formation of higher-functionalized RO_2 radicals and the further formation of highly oxygenated molecules (HOMs) (Wang et al., 2017; Molteni et al., 2018). Self- or cross-reactions of RO_2 radicals were also found, leading to the formation of accretion products (R1c), especially HOM dimers, as well as RO, ROH and $R_{-H}O$ (R1a and b) (Berndt et al., 2018). However, the RH effects on the mechanism of *m*-xylene SOA formation are not well studied.

$$ROO\cdot + R'OO\cdot \rightarrow RO\cdot + R'O\cdot + O_2 \qquad (R1a)$$

$$\rightarrow ROH + R'_{-H}O + O_2 \qquad (R1b)$$

$$\rightarrow ROOR' + O_2 \qquad (R1c)$$

$$ROO\cdot + HOO\cdot \rightarrow RO\cdot + HO\cdot + O_2 \qquad (R2a)$$

$$\rightarrow ROOH + O_2 \qquad (R2b)$$

RH effects on SOA formation from *m*-xylene under low NO_x condition have not been studied well. In the present study, we present the results from the experiments about the SOA formation from the OH-initiated oxidation of *m*-xylene in the absence of seed particles in a smog chamber. Both the SOA yields and chemical components under both low and high RH conditions will be reported. The underlying mechanism of SOA formation for these different conditions will be also discussed.

2 Experimental materials and methods

2.1 Equipment and reagents

Experiments of *m*-xylene photooxidation were performed in a 1 m^3 Teflon FEP film reactor (DuPont 500A, USA) in an indoor smog chamber, which is similar to our previous works (Jia and Xu, 2014, 2016, 2018; Ge et al., 2016, 2017c, a, b). So only a brief introduction is presented here. A light source was provided by 96 lamps (F40BLB, GE; UVA-340, Q-Lab, USA) inside the chamber to simulate the UV band of solar spectrum in the troposphere. The NO_2 photolysis rate was determined to be 0.23 min^{-1}, which was used to reflect the light intensity in the reactor. To remove the electric charge on the surface of the FEP reactor, two ionizing air blowers were equipped in the chamber and were used throughout each experiment.

The background gas was zero air, which was generated from Zero Air Supply and CO Reactor (Model 111 and 1150, Thermo Scientific, USA) and further purified by hydrocarbon traps (BHT-4, Agilent, USA). The desired RH in the reactor was obtained by bubbling dry zero air through ultrapure water (Milli Q, 18MU, Millipore Ltd., USA). The RH and temperature in the reactor were measured by a hygrometer (Model 645, Testo AG, Germany).

Throughout each experiment, the background NO_x concentration in the reactor was lower than 1 ppb and OH radicals were provided from H_2O_2 photolysis. Hydrogen peroxide was introduced to the reactor by evaporating a measured volume of H_2O_2 solution (30 wt %) into a zero air stream over a period of 30 min to the desired concentration of 20 ppm. Though the H_2O_2 level was not measured, it was estimated through the measured volume of H_2O_2 solution evaporated. *m*-Xylene (99%, Alfa Aesar) was introduced to the reactor subsequently using the same approach. No seed particles were introduced artificially. The experiments were conducted for 4 h.

2.2 Monitoring and analysis

The concentration of *m*-xylene in the reactor was measured with a gas chromatograph-mass spectrometer (GC-MS, Model 7890A GC and Model 5975C mass selective detector, Agilent, USA), which was equipped with a thermal desorber (Master TD, Dani, Italy). The size distribution and concentrations of particles were monitored with a scanning mobility particle sizer (SMPS, Model 3936, TSI, USA). The particle wall loss constant has been determined to be 3.0×10^{-5} s^{-1} at low RH and 6.0×10^{-5} s^{-1} at high RH conditions. The particles measured by SMPS consisted of liquid water content (LWC) and SOA at certain RH conditions. To determine the SOA concentration, LWC was determined at the end of each high RH experiment, which was based on the method in a previous study (Jia and Xu, 2018). Thus, here a brief introduction is only given. After the lights were turned off in high RH experiments, the SMPS was modified to the dry mode through adding a Nafion dryer (Perma Pure MD-700-12F-3) to the sampling flow and a Nafion dryer (Perma Pure PD-200T-24MPS) to the sheath flow, leading to the reduction of RH in the sample air to 10 % and that in the sheath to 7 %. After modifying to the dry mode, the humid air in SMPS was quickly replaced by dry air through venting the sheath air at 5 L min-1, and then the dry aerosol was measured by SMPS. The LWC was determined by the difference of the particle mass concentrations before and after the modification of the dry mode.

For the analysis of functional groups of the chemical composition in SOA from *m*-xylene-OH irradiation, the SOA samples were collected and determined by FTIR (Fourier transform infrared spectrometer). The particles were collected on a ZnSe disk using a Dekati low-pressure impactor (DLPI, Dekati Ltd., Finland) at the end of each experiment (Ge et al., 2016; Jia and Xu, 2016). Then, the ZnSe disk was put in a FTIR (Nicolet iS10, Thermos Fisher, USA) for the measurement of functional groups of the chemical composition in SOA samples.

To obtain the detailed information of chemical composition, SOA particles were sampled using the Particle into Liquid Sampler (PILS, model 4001, BMI, USA). The flow rate of sample gas was around 11 L min^{-1}, and the output flow rate of liquid sample was 0.05 mL min^{-1}. Two denuders were used to remove the VOCs and acids in the sample gas. SOA liquid samples collected by PILS were finally transferred into vials for subsequent analysis. Operatively, the blank measurements were obtained by replacing the sample gas with zero air collected in vials. It is well known that the PILS samples water-soluble species in the SOA with high efficiency. In addition, it is reported that the PILS can also samples slightly water-soluble organic compounds with average O:C ratios higher than 0.26 instead of the total SOA composition and the collection efficiency could exceed 0.6 (Zhang et al., 2016). Thus, the PILS can sample the overwhelming majority of the SOA system in our study, though PILS cannot sample water-insoluble species in the SOA.

The accurate mass of organic compounds in SOA and their MS/MS fragmentations were measured by the ultrahigh performance liquid chromatograph (UPLC, Ultimate 3000, Thermo Scientific, USA)-heated-electrospray ionization-high-resolution orbitrap mass spectrometer (HESI-HRMS, Q Exactive, Thermo Scientific, USA). Methanol (Optima™ LC/MS Grade, Fisher Chemical, USA) was used as the eluent in UPLC system. The elution flow rate was 0.2 mL min^{-1}, and the overall run time was 5 minutes. The injection volume was 20 μL. The acquired mass spectrum of SOA was in the range of 80-1000 Da. The HESI source was conducted in both positive and negative ion modes using the optimum method for characterization of organic compounds. We used the Thermo Scientific Xcalibur software (Thermo Fisher Scientific Inc., USA) to analyse the data from HRMS. To calculate the elemental compositions of compounds, the accurate mass measurements were used. For further analysis of the data from the second stage of data-dependent mass spectrometry (ddMS^2), the Mass Frontier program (Version 7.0, Thermo Fisher Scientific Inc., USA) was used in order to simulate breaking the ions into fragments for comparison with the measured fragments to assist in identifying the structures. The reaction pathways and products of *m*-xylene-OH photooxidation in Master Chemical Mechanism (MCM v3.3.1, the website at http://mcm.leeds.ac.uk/MCM; last accessed October 16, 2017) was used for analysis of the products measured by HRMS (Jenkin et al., 2003; Jia and Xu, 2014).

3. Results and discussion

3.1 RH effects on SOA yields

Figure 1 shows the wall-loss-corrected particle mass concentration as a function of photooxidation reaction time for *m*-xylene-OH systems under both the low-RH and the high-RH conditions. It can be clearly seen that there is a large difference in the maximum mass concentration between low and high RHs. The maximum mass concentrations fitted are 150.3 and 95.5 μg m^{-3} at low RHs, whereas they are 21.0 and 7.5 μg m^{-3} at high RHs, with the largest difference being over ten times. The RH effect was reproducible when the initial *m*-xylene concentration was changed under similar conditions. To obtain the particle mass concentrations and SOA yield, an SOA density of 1.4 g cm^{-3} was used (Song et al., 2007). It should be noted that the fairly large scatter in the mass concentrations of SOA in Fig. 1 was observed, which mainly results from the uncertainty of SOA measurement by SMPS instrument. The interval of SOA data sampled by SMPS was 5 minutes, for which the sampling frequency was relatively low. SMPS measurement uncertainty is mainly dominated by size-dependent aerosol charging efficiency uncertainties and CPC sampling flow rate variability. The size-dependent aerosol charging efficiency is typically characterized by an accuracy of ± 10% (Jiang et al., 2014). The combination of various uncertainties, including SMPS measurement, sampling and even conversion of mass concentration from number concentration leads to the fairly large scatter in Fig. 1.

We used the definition of the ratio of the SOA mass to the consumed *m*-xylene mass to calculate the SOA yield at the end of each experiment. Under high RH condition, LWC accounts for a large proportion of particles (Jia and Xu, 2018). So, when SOA yield is calculated at high RH, the LWC has to be subtracted. The removal of aerosol water during the LWC measurement may cause the dissolved species that are probably volatile/semi-volatile compounds to evaporate back into the gas phase. Thus, SOA concentrations for high RH conditions were slightly underestimated, but the underestimation is extremely low and can be negligible.

Experimental conditions and SOA concentrations at the end of the experiments in *m*-xylene-OH oxidation system are summarized in Table 1. The SOA yields at low RH are 14.0-14.6%, while those at high RH are only around 0.8-2.2%. Both mass concentrations and SOA yields at low RH are an order of magnitude larger than those at high RH. It should be noticed that temperatures at high RH are slightly higher than those at low RH. Though low temperature can lead to a high SOA yield, the difference of temperature between low and high RH conditions in this study is lower than two degree, which cannot lead to a significantly different SOA yields to affect the result (Qi et al., 2010).

In the most recent study on toluene SOA formation conducted without seed particles (Hinks et al., 2018), the SOA yield at low NO_x level was 15% under dry conditions (< 2% RH) and 1.9% under humid conditions (89% RH), with the ratio of two yields between dry and humid conditions being over 7.5. The toluene SOA produced under high RH conditions were significantly suppressed, in which the tendency of RH effects on SOA yield was very similar with our study, though the difference of SOA yield between low and high RH conditions in Hinks et al (2018) was slightly smaller than that in this study. The small difference of RH effects between Hinks et al. and our study is likely associated with the difference in experimental conditions, including RHs and initial VOCs and H_2O_2 concentrations, in addition to different species. This comparison demonstrates that different species of toluene and *m*-xylene of aromatics pose very similar RH effects under low-NO_x conditions. Hinks et al. attributed the suppression of SOA yields by elevated RH to the lower level of oligomers generated by condensation reactions and the reduced mass loading at high RH. In a study on an SOA model for toluene oxidation, it could be found that the SOA yield at low NO_x level was 28-30% under low RH conditions (17-18% RH) and 20-25% under moderate RH conditions (48% RH) (Cao and Jang, 2010), but they did not focus on the RH effect to give an explanation. As the difference of RH was only ~30%, the RH effect on SOA yields was not as significant as those in Hinks et al and this study. Ng et al. have investigated the yields of SOA formed from *m*-xylene-OH system at low RH (4-6%) under low NO_x conditions (Ng et al., 2007). They obtained that the SOA yields were in the range of 35.2-40.4% in the presence of seed particles. The SOA yields were larger than that of this study, as they conducted the experiments under different irradiation time and with inorganic seed particles. These seed particles can provide not only surface for chemical reactions, but also acidic and aqueous environments that can promote the SOA formation (Jang et al., 2002; Liu et al., 2018; Faust et al., 2017). In a study on chemical oxidative potential of SOA (Tuet et al., 2017), it was observed that the concentration of SOA from *m*-xylene irradiation at low NO_x level under dry condition was much larger than that under humid condition (89.3 $\mu g\ m^{-3}$ at < 5% RH and 13.9 $\mu g\ m^{-3}$ at 45% RH), but they did not calculate the *m*-xylene SOA yields or give an explanation for the RH effect. However, a previous study under high NO_x conditions (Zhou et al., 2011) found that the effect of RH on

SOA yields from aromatics photooxidation were positive, which obtained opposite results to our study. LWC was used to account for this positive effect as it could promote SOA formation through aqueous chemistry (Jia and Xu, 2014; Wang et al., 2016; Faust et al., 2017; Liu et al., 2018).

It should be noted that seed aerosols were not artificially introduced throughout all the experiments, which could lead to the underestimation of SOA, as SOA-forming vapours partly condense to the chamber walls instead of particles (Matsunaga and Ziemann, 2010; Zhang et al., 2014). The extent to which vapor wall deposition affects SOA mass yields depends on the specific parent hydrocarbon system (Zhang et al., 2014; Zhang et al., 2015; Nah et al., 2016; Nah et al., 2017). Zhang et al (2014) have estimated two *m*-xylene systems under low NO_x conditions and concluded that SOA mass yields were underestimated by factors of 1.8 (Ng et al., 2007) and 1.6 (Loza et al., 2012) under low RH conditions. In addition, the excess use of H_2O_2 can lead to an excess OH radicals, leading to a less underestimation of SOA formation as the losses of SOA-forming vapours can be mitigated via the use of excess oxidant concentrations (Nah et al., 2016). Thus, the underestimation of SOA formation can be limited. In fact, the wall loss of *m*-xylene was not taken into consideration of calculation of mass yields, which generally overestimates the mass yields.

The wall loss of chemical species that is sensitive to humidity may affect the RH effect on SOA yields, as the reduction of SOA yields at the high humidity may be due to the chemical loss to the wet chamber wall. To estimate the extent of how much the wall loss of chemical species affects the SOA formation at different RHs, we take glyoxal and acetone as reference compounds. Glyoxal, a typical compound that can form SOA, can easily dissolve in the aqueous phase due to the large Henry's law constant of 4.19×10^5 M atm^{-1} (Ip et al., 2009), very sensitive to humidity. Loza et al. (2010) found that the wall loss of glyoxal was minimal at 5% RH, with $k_W = 9.6 \times 10^{-7}$ s^{-1}, whereas k_W was 4.7×10^{-5} s^{-1} at 61% RH. We assume that k_W linearly increases with RH, and the k_W value is estimated to be 6.1×10^{-5} s^{-1} at 80% and 7.4×10^{-6} at 13% RH, with the difference being 8.2 times. According to the wall loss of glyoxal, glyoxal only decreased by 10% at the end of our experiment at low RH, while glyoxal decreased by 59% at high RH. Acetone can hardly dissolve in the aqueous phase due to the small Henry's law constant of 29 M atm^{-1} (Poulain et al., 2010), which is 4 orders of magnitude less than that of glyoxal. Ge et al. (2017) obtained that the wall loss of acetone was 5.0×10^{-6} s^{-1} at 87% RH and 3.3×10^{-6} s^{-1} at 5% RH, with a factor of 1.5. The difference of wall loss between glyoxal and acetone at low RH is about 2 times, while it becomes about 12 times at high RH. Thus, it can be considered that the wall loss among different species at low RH is less affected by the Henry's law constant, but it is greatly affected at high RH. In our study glycolaldehyde (See the Sec. 3.3) is found to be an important SOA precursor that can form a large fraction of oligomers in our experiments, but the wall loss of glycolaldehyde is not available. The Henry's law constant of glycolaldehyde was obtained to be 4.14×10^4 M atm^{-1} (Betterton and Hoffmann, 1988), an order of magnitude lower than glyoxal, indicating that glycolaldehyde is less sensitive to humidity than glyoxal but much more sensitive to humidity than acetone. Based on the data of these two reference species, the wall loss of glycolaldehyde at low RH is taken to be 5×10^{-6} s^{-1}, and the difference in wall loss between high and low RHs is about 6 times. Then, the wall loss of glycolaldehyde at high RH can be 3×10^{-5} s^{-1}. Then, it is estimated that glycolaldehyde would decrease by 7% at low RH and by 35% at high RH at the end of our experiment, respectively. This means that SOA yield would be underestimated by 35% at high RH and by 7% at low RH if glycolaldehyde lost to the wall was completely transformed to SOA. If this wall effect of SOA precursors was taken into consideration, the SOA yields at high (Exp. 3) and low (Exp. 2) RHs would be 3.4% and 15.1%, respectively. Alternatively, the SOA yield at high RH was underestimated to be 42% relative to that at low RH. Even the sensitivity of the wall loss to RH was taken to be 8 times, the SOA yield at high RH would be underestimated to be 62% compared to that at low RH. In fact, there were many different SOA precursors from the *m*-xylene oxidation system that probably have much smaller Henry's law constant relative to that of glycolaldehyde. Thus, it is concluded that the RH effect on SOA formation from *m*-xylene oxidation by H_2O_2 without NO_x is negative.

3.2 RH effects on functional groups of SOA

Figure 2 shows the FTIR spectra of particles from the photooxidation of *m*-xylene-OH experiments under both low (Exp. 2) and high (Exp. 3) RH conditions. The DLPI sample flow rate was 10 L min^{-1}, and the sampling duration was 15 min. We used same sampling flow rate and duration for both RH conditions. DLPI has 13 stages, and it can collect particles in the size range of 30 nm - 10 mm. When we sampled using DLPI, the four plates for stages 4-7 were removed, so that particles in the range of 108-650 nm were collected on the third plate. As shown in Fig. S2 in the supplementary information, the particles in the range of 108-650 nm can represent the total SOA from *m*-xylene oxidation in this study. The mean collection efficiency of the DLPI was 83% for stages 4-7 (Durand et al., 2014). Thus, the SOA mass collected on the ZnSe window was 10.3 and 3.0 μg at low RH (Exp. 2) and high RH (Exp. 3), based on the SMPS measurement and the DLPI collection efficiency. As shown in Fig. 2, the SOA from *m*-xylene-OH experiments can be obviously observed under both two RH conditions. The intensities of all functional groups from the low RH experiment are much higher than those from the high RH experiment, which is consistent with the reduced SOA yields under elevated RH conditions.

The assignment and the intensity of the FTIR absorption frequencies is summarized in Table 2. The broad absorption at 3600-2400 cm^{-1} is O-H stretching vibration in phenol, hydroxyl and carboxyl groups. The sharp absorption at 1720 cm^{-1} is the C=O stretching vibration in carboxylic acids, formate esters, aldehydes and ketones. The absorptions at 1605 cm^{-1} match the bending vibration of liquid water. The absorptions at 1415 cm^{-1} match the deformation of CO-H, phenolic O-H and C-O. The absorptions at 1180 cm^{-1} match the C-O-C stretching of polymers, C-O and OH of COOH groups. The absorptions at 1080 cm^{-1} match the C-C-OH stretching of alcohols.

The absorption intensity at ~3200 cm^{-1} that is identified as the hydroxyl group is used to be a representative for reflection of the SOA formation. As well, Table 2 gives the ratio of intensities at high RH to those at low RH to compare the difference of relative intensities of functional groups. The intensities of functional groups are obviously suppressed at high RH, but the extents of the suppression for different functional groups are basically divided into two types. The ratios of O-H, C-H, C=O and C-C-OH groups are 0.29 to 0.34, which is close to the ratio of SOA mass at high RH to that at low RH collected on the ZnSe disk, whereas the ratios of CO-H, C-O-C, C-O-H in COOH are above 0.48. The relative intensity of the C-O-C group is significantly higher than the C=O group, which can be explained by more oligomerization with the formation of C-O-C than other reactions at high RH. Nevertheless, the FTIR results cannot provide further information to well explain the differences of SOA yields between low and high RH, which will be further discussed in terms of mass spectra of SOA in the next section.

3.3 RH effects on mass spectra of SOA

We selected the sample mass spectra whose intensities are larger than 10^5 under the low RH condition and corresponding mass spectra under the high RH condition, followed by the blank mass spectra deduction. The blank-deducting mass spectra of SOA formed from *m*-xylene-OH photooxidation under low and high RH conditions in both positive and negative ion modes are presented in Fig. 3, which is plotted as a function of the mass-to-charge ratio. It should be noted that the Y-axis scales for low and high RH are largely different, 10^6 at low RH and 10^5 at high RH. As shown in Fig. 3, a visible decrease in the overall peak intensities for both positive and negative ion modes can be obviously observed as the RH elevates, which is consistent with the result that the SOA mass concentration is lower at high RH. In addition, it is obvious that the number of peaks is less under the high RH condition. As shown in Fig. 3, where the m/z values of SOA samples are close for both low and high conditions, the absolute and relative intensities of the peaks are much different, indicating that RH significantly affects the concentration of SOA components.

Table 3 lists the peaks whose intensities are larger than 10^6 of low RH samples and the structure can be proposed according to the gas-phase chemical mechanism of *m*-xylene-OH photooxidation included in MCM and the fragments from MS/MS analysed with Mass Frontier. In the positive ion mode, an $[M+H]^+$ ion of m/z = 137.05962 at low RH and 137.05931 at high RH is assigned as a molecular ion formula of $C_8H_9O_2^+$ that has a mass difference of $\Delta = 0.6$ and 1.0 mDa for low and high RH, respectively. The structure of identified compound $C_8H_8O_2$ is proposed to be 2,6-dimethyl-1,4-benzoquinone, the fragments of which from MS/MS match those from simulation of the Mass Frontier program. This compound was also identified and quantified in a previous study on SOA compositions from *m*-xylene-NO_x irradiation using the method of GC-MS analysis with authentic standards (Forstner et al., 1997). Thus, 2,6-dimethyl-1,4-benzoquinone was the SOA component partitioning into particle phase from the gas phase. The measured ion of m/z = 155.07013 at low RH and 155.06985 at high RH is assigned as a molecular ion formula of $C_8H_{11}O_3^+$ that has $\Delta = 1.2$ and 1.5 mDa, and its structure is proposed to be O=CC1(C)OC1C=CC(=O)C, an oxidized unsaturated epoxide. The measured ion of m/z = 171.06509 at low RH and 171.06488 at high RH is assigned as a molecular ion formula of $C_8H_{11}O_4^+$ that has $\Delta = 1.2$ and 1.4 mDa, the structure of which is proposed to be a bicyclic peroxide. The measured ion of m/z = 187.06003 at low RH and 187.05678 at high RH is assigned as a molecular ion formula of $C_8H_{11}O_5^+$ that has $\Delta = 1.2$ and 4.4 mDa, whose structure is proposed to be O=CC1(C)OC1C(O)C(=O)C(=O)C. All these SOA components are suppressed to almost disappear at high RH, except for 2,6-dimethyl-1,4-benzoquinone.

For rough quantification of the RH effect, the peaks in Figure 3 were assigned with the number of carbon atoms. The intensities of the peaks with the same number of carbon atoms (nC) are summed, which are presented in Figure 4. It should be noted that the Y-axis scales at low and high RHs are largely different, with a label step of 4.0×10^6 at low RH and 4.0×10^5 at high RH in the positive ion mode, 5.0×10^6 at low RH and 1.0×10^5 at high RH in the negative ion mode. The compounds with nC > 8, larger number of carbon atoms than *m*-xylene, are proposed to be oligomers that account for a large mass fraction of SOA due to their large molecular weights and lower volatilities, though their peak intensities are lower. As a result, the processes for formation of such compounds play an important role in the formation of SOA. It can be obviously observed that the peak intensities are much lower at high RH in the negative ion mode than that in the positive mode, indicating that the decrease of the compounds obtained in the negative ion mode account for a larger decrease at high RH. Moreover, in the positive ion mode, compounds with nC > 8, especially those with nC > 10, account for more SOA mass at high RH than at low RH, which can be observed by the increase of relative intensities of oligomers. However, in the negative ion mode, compounds with nC > 8 account for less SOA mass at high RH. In the positive ion mode, 15 compounds with nC = 10 identified with HRMS dominate the spectrum. To get more information, the MS/MS data analysis was further carried out. We found that the fragment with m/z = 61.03 obtained by the MS/MS was observed in nine out of the fifteen compounds, which is assigned as a molecular ion formula of $C_2H_5O_2^+$. The sum of peak intensities of these nine compounds accounts for about 70% of the sum of peak intensities of these fifteen nC = 10 compounds. The structure of this fragment is possibly proposed to be glycolaldehyde ($C_2H_4O_2$), which has been observed previously in the oxidation of *m*-xylene (Cocker et al., 2001). It has been implied that the oligomerization of glycolaldehyde took place in the study of formation of toluene SOA (Hinks et al., 2018). This demonstrates that the nC = 10 compounds are mainly from the oligomerization of glycolaldehyde and nC = 8 monomers.

3.4 Proposed mechanism of RH effects on SOA formation

It has been confirmed that glyoxal is an important SOA precursor via oligomerization (Jang et al., 2002; Kamens et al., 2011; Zhou et al., 2011). An explanation for the large difference of SOA yields and composition between low and high RH is proposed that water is directly involved in the chemical mechanism and further affects the SOA growth. However, in some particle-phase accretion equilibrium reactions, water is involved as a by-product. The elevated RH alters the equilibrium of reaction toward the decrease of products (Nguyen et al., 2011; Hinks et al., 2018). The hydrolysis of oligomers would be facilitated by the elevated RH after the oligomers are generated in gas phase and partition into particles with certain LWC. In this study and the previous study on toluene SOA formation, C_2H_2O was one of the most frequently mass difference at both RH, but the peak intensities of its relative compounds were much lower under elevated RH conditions (Hinks et al., 2018). C_2H_2O was proposed to be from the oligomerization reaction of glycolaldehyde ($C_2H_4O_2$), which can react with carbonyl compounds by aldol condensation reactions with water as the by-product. However, this mechanism cannot well explain the large different SOA yields at low and high RH.

Another possible explanation for RH effects on SOA chemical components is that RH influences the HOMs formation from *m*-xylene-OH system (Fig. 5). Reactions between *m*-xylene (C_8H_{10}) and OH radicals have two pathways, the H-abstraction from the methyl group and OH-addition to the aromatic ring, which generates products such as methylbenzaldehyde (C_8H_8O) and methylbenzyl alcohol ($C_8H_{10}O$), as shown in Scheme 1. OH-addition is the dominant pathway, as the branching ratio of H-abstraction only accounts for 4% based on the MCM simulation. OH-addition to the aromatic ring is followed by O_2-

adduct and isomerization to form a carbon-centered radical, which can form a dimethylphenol ($C_8H_{10}O$) or is adducted by an O_2 molecule forming a bicyclic peroxy radical (BPR, $C_8H_{11}O_5$) (Calvert et al., 2002; Birdsall et al., 2010; Wu et al., 2014), which is called the RO_2 autoxidation. The BPR reacts with other RO_2 radicals or HO_2 forming the bicyclic oxy radical ($C_8H_{11}O_4$). This RO radical can get further reaction and finally form carbonylic products (R1a and R2a), such as (methyl) glyoxal and other SOA precursors (Jenkin et al., 2003; Hallquist et al., 2009; Carlton et al., 2010; Carter and Heo, 2013), or react with HO_2 radicals forming bicyclic hydroxyhydroperoxides (ROOH, $C_8H_{12}O_5$) (R2b), or react with other RO_2 radicals forming ROH ($C_8H_{12}O_4$) and $R_{-H}O$ ($C_8H_{10}O_4$) (R1b). The self- and cross-reactions of RO_2 radicals also form ROOR ($C_{16}H_{22}O_{10}$) or ROOR' that is the accretion products (Berndt et al., 2018; Molteni et al., 2018). The further autoxidation of BPR can form a highly-functionalized RO_2 radicals and further get reacted and finally form HOMs (Types 1 and 2 in Scheme 1) (Wang et al., 2017; Crounse et al., 2013; Ehn et al., 2014; Jokinen et al., 2015; Berndt et al., 2016). Dimethylphenol ($C_8H_{10}O$) as well as other products from termination reaction with benzene ring or double bond can react with OH radicals and get further reacted to form HOMs as well. The compounds with the number below their formulae in scheme 1 were determined by HRMS to be present in the particle phase.

The distribution of relative intensity of SOA products with same carbon number was shown in Fig. 5 to investigate the potential RH effect on HOMs. Oxidation compounds with the same carbon number but different oxygen number were observed. In the mass-to-charge (m/z) range 135-240 Da in both positive and negative ion modes, the oxidation products contain the carbon skeleton of *m*-xylenes (monomer region, nC = 8), while in the m/z range 320-410 Da the number of carbon atoms is doubled (dimer region, nC = 16). The compounds with high O/C ratios are observed, which are generally called HOMs. In a previous study on *m*-xylene oxidation, HOM monomers including $C_8H_{10}O_{5-8}$, $C_8H_{12}O_{5-8}$ and $C_8H_{14}O_{6-8}$, and HOM dimers including $C_{16}H_{22}O_{9-12}$ and $C_{16}H_{24}O_{11}$ were obtained using CI-APi-TOF-MS (chemical ionization atmospheric pressure interface time of flight mass spectrometer) (Molteni et al., 2018), which are also determined in our study. More HOMs can be obtained in the negative ion mode where oxygen atom numbers can reach up to 8 for monomers and 12 for dimers, when compared with those in the positive ion mode. In addition, here the O/C ratio was calculated based on the O and C atom numbers in structures and peak intensities, which is 0.57 and 0.71 in the positive and negative ion modes, respectively. This also demonstrates that the compounds in the negative ion mode are much more oxygenated than those in the positive ion mode. As shown in Fig. 4, the peak intensities at high RH are much lower in the negative ion mode than in the positive mode, indicating that the decrease of the more oxygenated compounds account for the larger fraction at high RH. These high O/C ratios cannot be explained by any of the formerly known oxidization pathways except that RO_2 autoxidation is taken into consideration (Crounse et al., 2013; Barsanti et al., 2017). Both HOM monomers and dimers obviously decrease with increasing RH. RH significantly affect the formation of the HOMs. The relative intensities of compounds with same nC but larger oxygen number decrease more significantly. High RH significantly suppresses the more oxidized compounds whose volatility is lower and molecular weights are larger. Therefore, it is considered that RH suppresses the RO_2 autoxidation and further affects the SOA yield.

The wall process of the reactor enlarges the difference of SOA mass between low and high RH. The wall loss of some chemical species is faster at high RH, which leads to the reduction of SOA yield. In addition, the difference of SOA mass can be also enhanced based on the gas to particle partitioning rule (Li et al., 2018).

4. Conclusion and atmospheric implication

The current study investigates the effect of RH on SOA formation from the oxidation of *m*-xylene under low NO_x conditions in the absence of seed particles. The elevated RH can significantly obstruct the SOA formation from the *m*-xylene-OH system, so that the SOA yield decrease from 13.8% at low RH to 0.8% at high RH, with a significant discrepancy of higher than one order of magnitude. The FTIR results of functional groups show the relative increase of the C-O-C group at high RH as compared with low RH, indicating that the oligomers from carbonyl compounds cannot well explain the suppression of SOA yield. HOMs were observed to be suppressed in the HRMS spectra. The chemical mechanism for explaining the obvious difference of RH effects on SOA formation from *m*-xylene-OH system has been proposed based on the analysis of both FTIR and HRMS measurements as well as MCM simulations. The reduced SOA at high RH is mainly ascribed to the less formation of oligomers and the suppression of RO_2 autoxidation. Together with the previous study on toluene SOA, it is conceivable that the effect of RH on SOA yield is a common feature of SOA formation from aromatics oxidation under low NO_x conditions and using H_2O_2 as the OH radical source. Our results obviously indicate that the production of SOA from aromatics in low-NO_x environments can be strongly modulated by the ambient RH probably due to the influence of H_2O on the formation of HOMs and oligomers. Our study highlights the role of water in the SOA formation, which is particularly related to chemical mechanisms used to explain observed air quality and to predict chemistry in air quality models and climate models. The clear pathway of the influence of H_2O on the formation of HOMs needs to be further studied in the future.

Author contribution

Qun Zhang and Yongfu Xu designed the research. Qun Zhang carried out the experiments and analyzed the data. Long Jia provided valuable advices on the experiment operations. Yongfu Xu and Long Jia provided advices on the analysis of results. Qun Zhang prepared the manuscript with contributions from all co-authors.

Acknowledgments

This work was supported by the National Key R&D Program of China (2017YFC0210005) and National Natural Science Foundation of China (No. 41375129).

References

Barsanti, K. C., Kroll, J. H., and Thornton, J. A.: Formation of low-volatility organic compounds in the atmosphere: Recent advancements and insights, J. Phys. Chem. Lett., 8, 1503-1511, 10.1021/acs.jpclett.6b02969, 2017.

Berndt, T., Richters, S., Jokinen, T., Hyttinen, N., Kurten, T., Otkjaer, R. V., Kjaergaard, H. G., Stratmann, F., Herrmann, H., Sipila, M., Kulmala, M., and Ehn, M.: Hydroxyl radical-induced formation of highly oxidized organic compounds, Nat. Commun., 7, 13677, 10.1038/ncomms13677, 2016.

Berndt, T., Scholz, W., Mentler, B., Fischer, L., Herrmann, H., Kulmala, M., and Hansel, A.: Accretion product formation from self- and cross-reactions of RO_2 radicals in the atmosphere, Angew. Chem. Int. Ed., 57, 3820-3824, 10.1002/anie.201710989, 2018.

Betterton, E. A., and Hoffmann, M. R.: Henry's law constants of some environmentally important aldehydes, Environ. Sci. Technol., 22, 1415-1418, 10.1021/es00177a004, 1988.

Birdsall, A. W., Andreoni, J. F., and Elrod, M. J.: Investigation of the role of bicyclic peroxy radicals in the oxidation mechanism of toluene, J. Phys. Chem. A, 114, 10655-10663, 10.1021/jp105467e, 2010.

Bloss, C., Wagner, V., Jenkin, M. E., Volkamer, R., Bloss, W. J., Lee, J. D., Heard, D. E., Wirtz, K., Martin-Reviejo, M., Rea, G., Wenger, J. C., and Pilling, M. J.: Development of a detailed chemical mechanism (MCMv3.1) for the atmospheric oxidation of aromatic hydrocarbons, Atmos. Chem. Phys., 5, 641-664, 10.5194/acp-5-641-2005, 2005.

Calvert, J. G., Atkinson, R., Becker, K. H., Kamens, R. M., Seinfeld, J. H., Wallington, T. H., and Yarwood, G.: The mechanisms of atmospheric oxidation of the aromatic hydrocarbons, Oxford University Press, 2002.

Cao, G., and Jang, M.: An SOA model for toluene oxidation in the presence of inorganic aerosols, Environ. Sci. Technol., 44, 727-733, 10.1021/es901682r, 2010.

Carlton, A. G., Bhave, P. V., Napelenok, S. L., Edney, E. O., Golam, S., Pinder, R. W., Pouliot, G. A., and Marc, H.: Model representation of secondary organic aerosol in CMAQv4.7, Environ. Sci. Technol., 44, 8553-8560, 10.1021/es100636q, 2010.

Carter, W. P. L., and Heo, G.: Development of revised SAPRC aromatics mechanisms, Atmos. Environ., 77, 404-414, 10.1016/j.atmosenv.2013.05.021, 2013.

Cocker, D. R., Mader, B. T., Kalberer, M., Flagan, R. C., and Seinfeld, J. H.: The effect of water on gas-particle partitioning of secondary organic aerosol: II. *m*-xylene and 1,3,5-trimethylbenzene photooxidation systems, Atmos. Environ., 35, 6073-6085, 10.1016/s1352-2310(01)00405-8, 2001.

Crounse, J. D., Nielsen, L. B., Jørgensen, S., Kjaergaard, H. G., and Wennberg, P. O.: Autoxidation of organic compounds in the atmosphere, J. Phys. Chem. Lett., 4, 3513-3520, 10.1021/jz4019207, 2013.

Ding, X., Wang, X.-M., Gao, B., Fu, X.-X., He, Q.-F., Zhao, X.-Y., Yu, J.-Z., and Zheng, M.: Tracer-based estimation of secondary organic carbon in the Pearl River Delta, south China, J. Geophys. Res., 117, D05313, 10.1029/2011jd016596, 2012.

Durand, T., Bau, S., Morele, Y., Matera, V., Bémer, D., and Rousset, D.: Quantification of low pressure impactor wall deposits during zinc nanoparticle sampling, Aerosol Air Qual. Res., 14, 1812-1821, 10.4209/aaqr.2013.10.0304, 2014.

Ehn, M., Thornton, J. A., Kleist, E., Sipilä, M., Junninen, H., Pullinen, I., Springer, M., Rubach, F., Tillmann, R., and Lee, B.: A large source of low-volatility secondary organic aerosol, Nature, 506, 476-479, 10.1038/nature13032, 2014.

Faust, J. A., Wong, J. P. S., Lee, A. K. Y., and Abbatt, J. P. D.: Role of aerosol liquid water in secondary organic aerosol formation from volatile organic compounds, Environ. Sci. Technol., 51, 1405-1413, 10.1021/acs.est.6b04700, 2017.

Finlayson-Pitts, B. J., and Pitts Jr., J. N.: Chapter 6-Rates and mechanisms of gas-phase reactions in irradiated organic-NO_x-air mixtures, in: Chemistry of the Upper and Lower Atmosphere, Academic Press, San Diego, 179-263, 2000.

Forstner, H. J. L., Flagan, R. C., and Seinfeld, J. H.: Secondary organic aerosol from the photooxidation of aromatic hydrocarbons: Molecular composition, Environ. Sci. Technol., 31, 1345-1358, 10.1021/es9605376, 1997.

Ge, S., Xu, Y., and Jia, L.: Secondary organic aerosol formation from ethyne in the presence of NaCl in a smog chamber, Environ. Chem., 13, 699-710, 10.1071/en15155, 2016.

Ge, S., Xu, Y., and Jia, L.: Secondary organic aerosol formation from propylene irradiations in a chamber study, Atmos. Environ., 157, 146-155, 10.1016/j.atmosenv.2017.03.019, 2017a.

Ge, S., Xu, Y., and Jia, L.: Secondary organic aerosol formation from ethylene ozonolysis in the presence of sodium chloride, J. Aerosol Sci., 106, 120-131, 10.1016/j.jaerosci.2017.01.009, 2017b.

Ge, S., Xu, Y., and Jia, L.: Effects of inorganic seeds on secondary organic aerosol formation from photochemical oxidation of acetone in a chamber, Atmos. Environ., 170, 205-215, 10.1016/j.atmosenv.2017.09.036, 2017c.

Hallquist, M., Wenger, J. C., Baltensperger, U., Rudich, Y., Simpson, D., Claeys, M., Dommen, J., Donahue, N. M., George, C., Goldstein, A. H., Hamilton, J. F., Herrmann, H., Hoffmann, T., Iinuma, Y., Jang, M., Jenkin, M. E., Jimenez, J. L., Kiendler-Scharr, A., Maenhaut, W., McFiggans, G., Mentel, T. F., Monod, A., Prévôt, A. S. H., Seinfeld, J. H., Surratt, J. D., Szmigielski, R., and Wildt, J.: The formation, properties and impact of secondary organic aerosol: current and emerging issues, Atmos. Chem. Phys., 9, 5155-5236, 10.5194/acp-9-5155-2009, 2009.

Hansen, J. E., and Sato, M.: Trends of measured climate forcing agents, Proc. Natl. Acad. Sci. U. S. A., 98, 14778-14783, 10.1073/pnas.261553698, 2001.

Healy, R. M., Temime, B., Kuprovskyte, K., and Wenger, J. C.: Effect of relative humidity on gas/particle partitioning and aerosol mass yield in the photooxidation of *p*-xylene, Environ. Sci. Technol., 43, 1884-1889, 10.1021/es802404z, 2009.

Hinks, M. L., Montoya-Aguilera, J., Ellison, L., Lin, P., Laskin, A., Laskin, J., Shiraiwa, M., Dabdub, D., and Nizkorodov, S. A.: Effect of relative humidity on the composition of secondary organic aerosol from the oxidation of toluene, Atmos. Chem. Phys., 18, 1643-1652, 10.5194/acp-18-1643-2018, 2018.

Huang, R. J., Zhang, Y., Bozzetti, C., Ho, K. F., Cao, J. J., Han, Y., Daellenbach, K. R., Slowik, J. G., Platt, S. M., Canonaco, F., Zotter, P., Wolf, R., Pieber, S. M., Bruns, E. A., Crippa, M., Ciarelli, G., Piazzalunga, A., Schwikowski, M., Abbaszade, G., Schnelle-Kreis, J., Zimmermann, R., An, Z., Szidat, S., Baltensperger, U., El Haddad, I., and Prevot, A. S.: High secondary aerosol contribution to particulate pollution during haze events in China, Nature, 514, 218-222, 10.1038/nature13774, 2014.

Ip, H. S. S., Huang, X. H. H., and Yu, J. Z.: Effective Henry's law constants of glyoxal, glyoxylic acid, and glycolic acid, Geophys. Res. Lett., 36, L01802, 10.1029/2008gl036212, 2009.

Jacobson, M. C., Hansson, H. C., Noone, K. J., and Charlson, R. J.: Organic atmospheric aerosols: Review and state of the science, Rev. Geophys., 38, 267-294, 10.1029/1998rg000045, 2000.

Jang, M., Czoschke, N. M., Lee, S., and Kamens, R. M.: Heterogeneous atmospheric aerosol production by acid-catalyzed particle-phase reactions, Science, 298, 814-817, 10.1126/science.1075798, 2002.

Jenkin, M. E., Saunders, S. M., Wagner, V., and Pilling, M. J.: Protocol for the development of the Master Chemical Mechanism, MCM v3 (Part B): tropospheric degradation of aromatic volatile organic compounds, Atmos. Chem. Phys., 3, 181-193, 10.5194/acp-3-181-2003, 2003.

Jia, L., and Xu, Y.: Effects of relative humidity on ozone and secondary organic aerosol formation from the photooxidation of benzene and ethylbenzene, Aerosol Sci. Technol., 48, 1-12, 10.1080/02786826.2013.847269, 2014.

Jia, L., and Xu, Y.: Ozone and secondary organic aerosol formation from Ethylene-NOx -NaCl irradiations under different relative humidity conditions, J. Atmos. Chem., 73, 81-100, 10.1007/s10874-015-9317-1, 2016.

Jia, L., and Xu, Y.: Different roles of water in secondary organic aerosol formation from toluene and isoprene, Atmos. Chem. Phys., 18, 8137-8154, 10.5194/acp-18-8137-2018, 2018.

Jiang, J., Kim, C., Wang, X., Stolzenburg, M. R., Kaufman, S. L., Qi, C., Sem, G. J., Sakurai, H., Hama, N., and McMurry, P. H.: Aerosol charge fractions downstream of six bipolar chargers: Effects of ion source, source activity, and flowrate, Aerosol Sci. Technol., 48, 1207-1216, 10.1080/02786826.2014.976333, 2014.

Jokinen, T., Sipilä, M., Richters, S., Kerminen, V. M., Paasonen, P., Stratmann, F., Worsnop, D., Kulmala, M., Ehn, M., and Herrmann, H.: Rapid autoxidation forms highly oxidized RO_2 radicals in the atmosphere, Angew. Chem. Int. Ed., 53, 14596-14600, 10.1002/anie.201408566, 2015.

Kamens, R. M., Zhang, H., Chen, E. H., Zhou, Y., Parikh, H. M., Wilson, R. L., Galloway, K. E., and Rosen, E. P.: Secondary organic aerosol formation from toluene in an atmospheric hydrocarbon mixture: Water and particle seed effects, Atmos. Environ., 45, 2324-2334, 10.1016/j.atmosenv.2010.11.007, 2011.

Kanakidou, M., Seinfeld, J. H., Pandis, S. N., Barnes, I., Dentener, F. J., Facchini, M. C., Dingenen, R. V., Ervens, B., Nenes, A., Nielsen, C. J., Swietlicki, E., Putaud, J. P., Balkanski, Y., Fuzzi, S., Horth, J., Moortgat, G. K., Winterhalter, R., Myhre, C. E. L., Tsigaridis, K., Vignati, E., Stephanou, E. G., and Wilson, J.: Organic aerosol and global climate modelling: a review, Atmos. Chem. Phys., 5, 1053-1123, 10.5194/acp-5-1053-2005, 2005.

Khoder, M. I.: Ambient levels of volatile organic compounds in the atmosphere of Greater Cairo, Atmos. Environ., 41, 554-566, 10.1016/j.atmosenv.2006.08.051, 2007.

Li, K., Li, J., Wang, W., Li, J., Peng, C., Wang, D., and Ge, M.: Effects of gas-particle partitioning on refractive index and chemical composition of *m*-xylene secondary organic aerosol, J. Phys. Chem. A, 122, 3250-3260, 10.1021/acs.jpca.7b12792, 2018.

Liu, T., Huang, D., Li, Z., Liu, Q., Chan, M., and Chan, C. K.: Comparison of secondary organic aerosol formation from toluene on initially wet and dry ammonium sulfate particles at moderate relative humidity, Atmos. Chem. Phys., 18, 5677-5689, 10.5194/acp-18-5677-2018, 2018.

Loza, C. L., Chhabra, P. S., Yee, L. D., Craven, J. S., Flagan, R. C., and Seinfeld, J. H.: Chemical aging of m-xylene secondary organic aerosol: laboratory chamber study, Atmos. Chem. Phys., 12, 151-167, 10.5194/acp-12-151-2012, 2012.

Matsunaga, A., and Ziemann, P. J.: Gas-wall partitioning of organic compounds in a Teflon film chamber and potential effects on reaction product and aerosol yield measurements, Aerosol Sci. Technol., 44, 881-892, 10.1080/02786826.2010.501044, 2010.

Molteni, U., Bianchi, F., Klein, F., El Haddad, I., Frege, C., Rossi, M. J., Dommen, J., and Baltensperger, U.: Formation of highly oxygenated organic molecules from aromatic compounds, Atmos. Chem. Phys., 18, 1909-1921, 10.5194/acp-18-1909-2018, 2018.

Nah, T., McVay, R. C., Zhang, X., Boyd, C. M., Seinfeld, J. H., and Ng, N. L.: Influence of seed aerosol surface area and oxidation rate on vapor wall deposition and SOA mass yields: a case study with α-pinene ozonolysis, Atmos. Chem. Phys., 16, 9361-9379, 10.5194/acp-16-9361-2016, 2016.

Nah, T., McVay, R. C., Pierce, J. R., Seinfeld, J. H., and Ng, N. L.: Constraining uncertainties in particle-wall deposition correction during SOA formation in chamber experiments, Atmos. Chem. Phys., 17, 2297-2310, 10.5194/acp-17-2297-2017, 2017.

Ng, N. L., Kroll, J. H., Chan, A. W. H., Chhabra, P. S., Flagan, R. C., and Seinfeld, J. H.: Secondary organic aerosol formation from *m*-xylene, toluene, and benzene, Atmos. Chem. Phys., 7, 3909-3922, 10.5194/acp-7-3909-2007, 2007.

Nguyen, T. B., Roach, P. J., Laskin, J., Laskin, A., and Nizkorodov, S. A.: Effect of humidity on the composition of isoprene photooxidation secondary organic aerosol, Atmos. Chem. Phys., 11, 6931-6944, 10.5194/acp-11-6931-2011, 2011.

Odum, J. R., Jungkamp, T. P., Griffin, R. J., Flagan, R. C., and Seinfeld, J. H.: The atmospheric aerosol-forming potential of whole gasoline vapor, Science, 276, 96-99, 10.1126/science.276.5309.96, 1997.

Offenberg, J. H., Lewis, C. W., Lewandowski, M., Jaoui, M., Kleindienst, T. E., and Edney, E. O.: Contributions of toluene and α-pinene to SOA formed in an irradiated toluene/α-pinene/NO_x/air mixture: comparison of results using ^{14}C content and SOA organic tracer methods, Environ. Sci. Technol., 41, 3972-3976, 10.1021/es070089+, 2007.

Poulain, L., Katrib, Y., Isikli, E., Liu, Y., Wortham, H., Mirabel, P., Le Calve, S., and Monod, A.: In-cloud multiphase behaviour of acetone in the troposphere: gas uptake, Henry's law equilibrium and aqueous phase photooxidation, Chemosphere, 81, 312-320, 10.1016/j.chemosphere.2010.07.032, 2010.

Qi, L., Nakao, S., Tang, P., and Cocker, D. R., III: Temperature effect on physical and chemical properties of secondary organic aerosol from *m*-xylene photooxidation, Atmos. Chem. Phys., 10, 3847-3854, 10.5194/acp-10-3847-2010, 2010.

Seinfeld, J. H., and Pandis, S. N.: Atmospheric chemistry and physics: From air pollution to climate change, 3rd ed., Wiley, Hoboken, 2016.

Song, C., Na, K., Warren, B., Malloy, Q., and Cocker, D. R., III: Secondary organic aerosol formation from *m*-xylene in the absence of NO_x, Environ. Sci. Technol., 41, 7409-7416, 10.1021/es070429r, 2007.

Spracklen, D. V., Jimenez, J. L., Carslaw, K. S., Worsnop, D. R., Evans, M. J., Mann, G. W., Zhang, Q., Canagaratna, M. R., Allan, J., Coe, H., McFiggans, G., Rap, A., and Forster, P.: Aerosol mass spectrometer constraint on the global secondary organic aerosol budget, Atmos. Chem. Phys., 11, 12109-12136, 10.5194/acp-11-12109-2011, 2011.

Tuet, W. Y., Chen, Y., Xu, L., Fok, S., Gao, D., Weber, R. J., and Ng, N. L.: Chemical oxidative potential of secondary organic aerosol (SOA) generated from the photooxidation of biogenic and anthropogenic volatile organic compounds, Atmos. Chem. Phys., 17, 839-853, 10.5194/acp-17-839-2017, 2017.

Wang, S., Wu, R., Berndt, T., Ehn, M., and Wang, L.: Formation of Highly Oxidized Radicals and Multifunctional Products from the Atmospheric Oxidation of Alkylbenzenes, Environ. Sci. Technol., 51, 8442-8449, 10.1021/acs.est.7b02374, 2017.

Wang, Y., Luo, H., Jia, L., and Ge, S.: Effect of particle water on ozone and secondary organic aerosol formation from benzene-NO_2-NaCl irradiations, Atmos. Environ., 140, 386-394, 10.1016/j.atmosenv.2016.06.022, 2016.

Warren, B., Song, C., and Cocker, D. R., III: Light intensity and light source influence on secondary organic aerosol formation for the *m*-xylene/NO_x photooxidation system, Environ. Sci. Technol., 42, 5461-5466, 10.1021/es702985n, 2008.

Wu, R., Pan, S., Li, Y., and Wang, L.: Atmospheric oxidation mechanism of toluene, J. Phys. Chem. A, 118, 4533-4547, 10.1021/jp500077f, 2014.

Zhang, X., Cappa, C. D., Jathar, S. H., McVay, R. C., Ensberg, J. J., Kleeman, M. J., and Seinfeld, J. H.: Influence of vapor wall loss in laboratory chambers on yields of secondary organic aerosol, Proc. Natl. Acad. Sci. U. S. A., 111, 5802-5807, 10.1073/pnas.1404727111, 2014.

Zhang, X., Schwantes, R. H., McVay, R. C., Lignell, H., Coggon, M. M., Flagan, R. C., and Seinfeld, J. H.: Vapor wall deposition in Teflon chambers, Atmos. Chem. Phys., 15, 4197-4214, 10.5194/acp-15-4197-2015, 2015.

Zhang, X., Dalleska, N. F., Huang, D. D., Bates, K. H., Sorooshian, A., Flagan, R. C., and Seinfeld, J. H.: Time-resolved molecular characterization of organic aerosols by PILS + UPLC/ESI-Q-TOFMS, Atmos. Environ., 130, 180-189, 10.1016/j.atmosenv.2015.08.049, 2016.

Zhao, Y., Saleh, R., Saliba, G., Presto, A. A., Gordon, T. D., Drozd, G. T., Goldstein, A. H., Donahue, N. M., and Robinson, A. L.: Reducing secondary organic aerosol formation from gasoline vehicle exhaust, Proc. Natl. Acad. Sci. U. S. A., 114, 6984-6989, 10.1073/pnas.1620911114, 2017.

Zhou, Y., Zhang, H., Parikh, H. M., Chen, E. H., Rattanavaraha, W., Rosen, E. P., Wang, W., and Kamens, R. M.: Secondary organic aerosol formation from xylenes and mixtures of toluene and xylenes in an atmospheric urban hydrocarbon mixture: Water and particle seed effects (II), Atmos. Environ., 45, 3882-3890, 10.1016/j.atmosenv.2010.12.048, 2011.

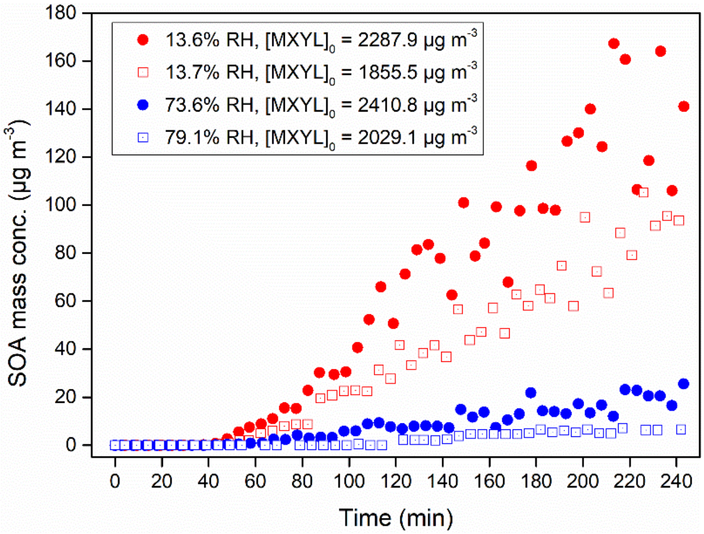

Figure 1. SOA mass concentrations as a function of irradiation time (corrected by particle wall loss).

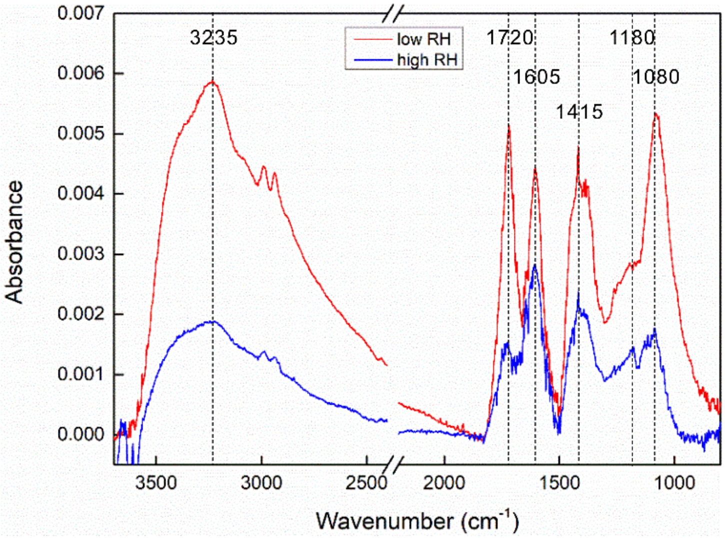

Figure 2. FTIR spectra of particles from photooxidation of *m*-xylene-OH experiments under low and high RH conditions.

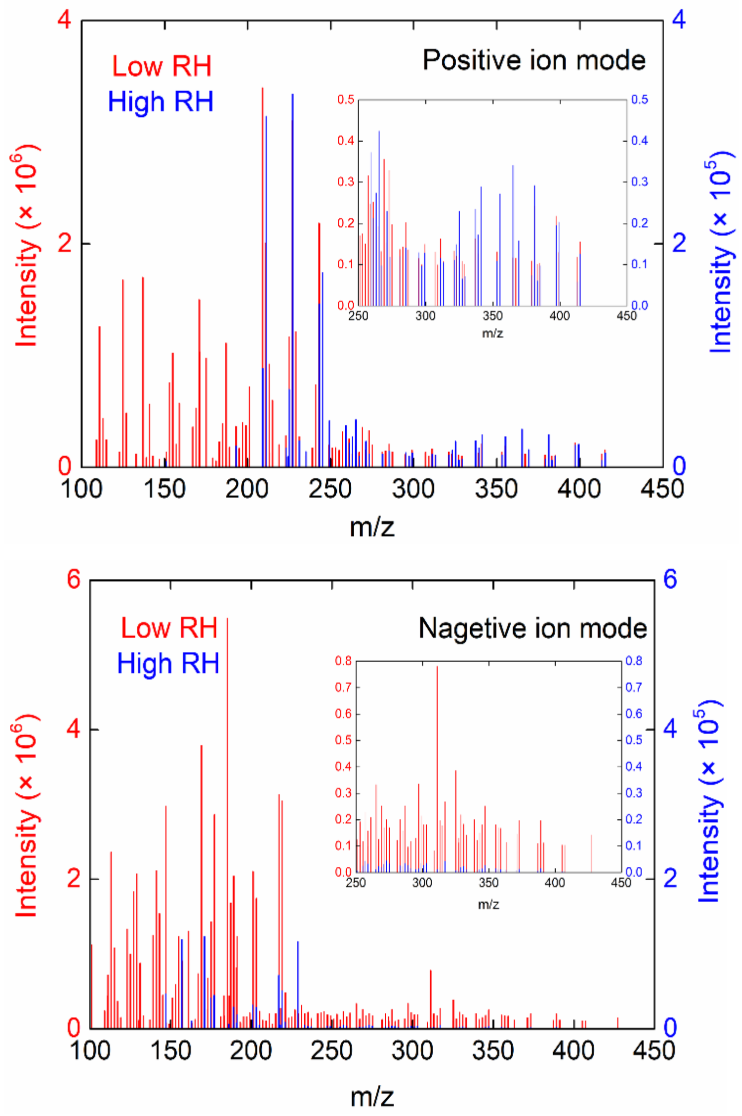

Figure 3. Selected background-subtraction HESI-Q Exactive-Orbitrap MS results of SOA in both positive and negative ion modes from the photooxidation of *m*-xylene-OH under both low and high RH conditions (Note that the Y-axis scales for low and high RH are largely different, 10^6 at low RH and 10^5 at high RH).

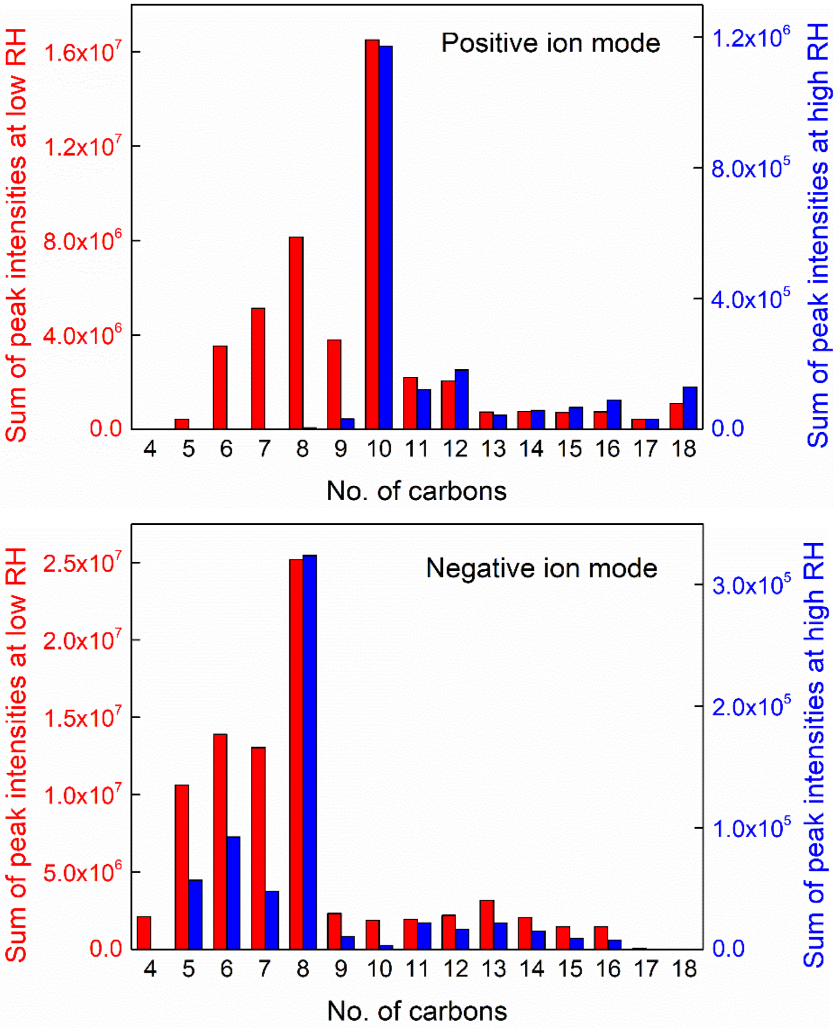

Figure 4. Sum of peak intensities based on peaks selected in Figure 3 as a function of the number of carbon atoms under the positive ion mode and negative ion mode (Note that the Y-axis scale at low and high RH are largely different, with a label step of 4.0 × 10^6 at low RH and 4.0 × 10^5 at high RH in the positive ion mode, 5.0 × 10^6 at low RH and 1.0 × 10^5 at high RH in the negative ion mode).

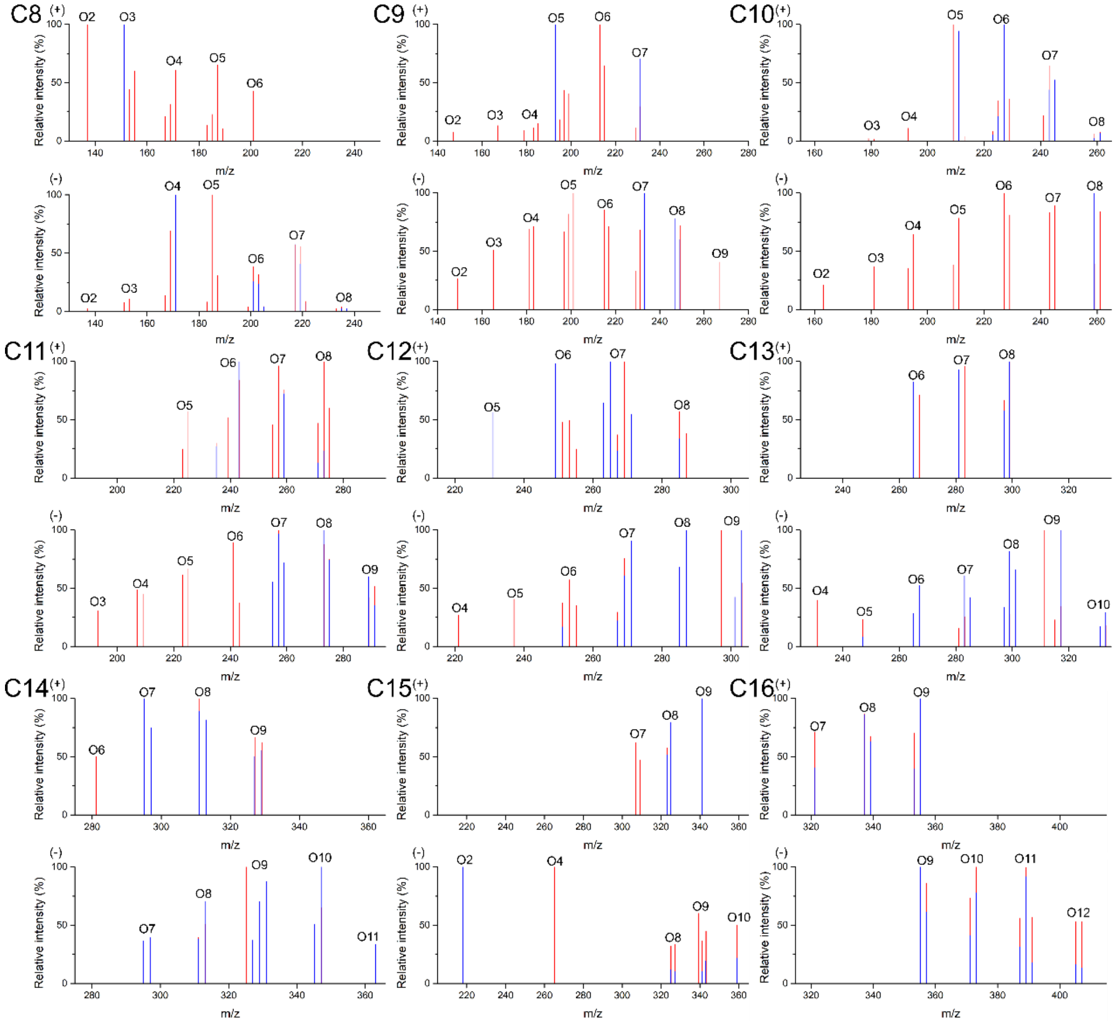

Figure 5. Mass spectra of SOA from *m*-xylene at both low (red) and high (blue) RH in the positive (+) and negative (-) ion modes, grouped with the same number of carbon atoms (from nC =8 to 16). On (n = 2, 3, ……, 12) means the number of oxygen atoms in the formula of the peak.

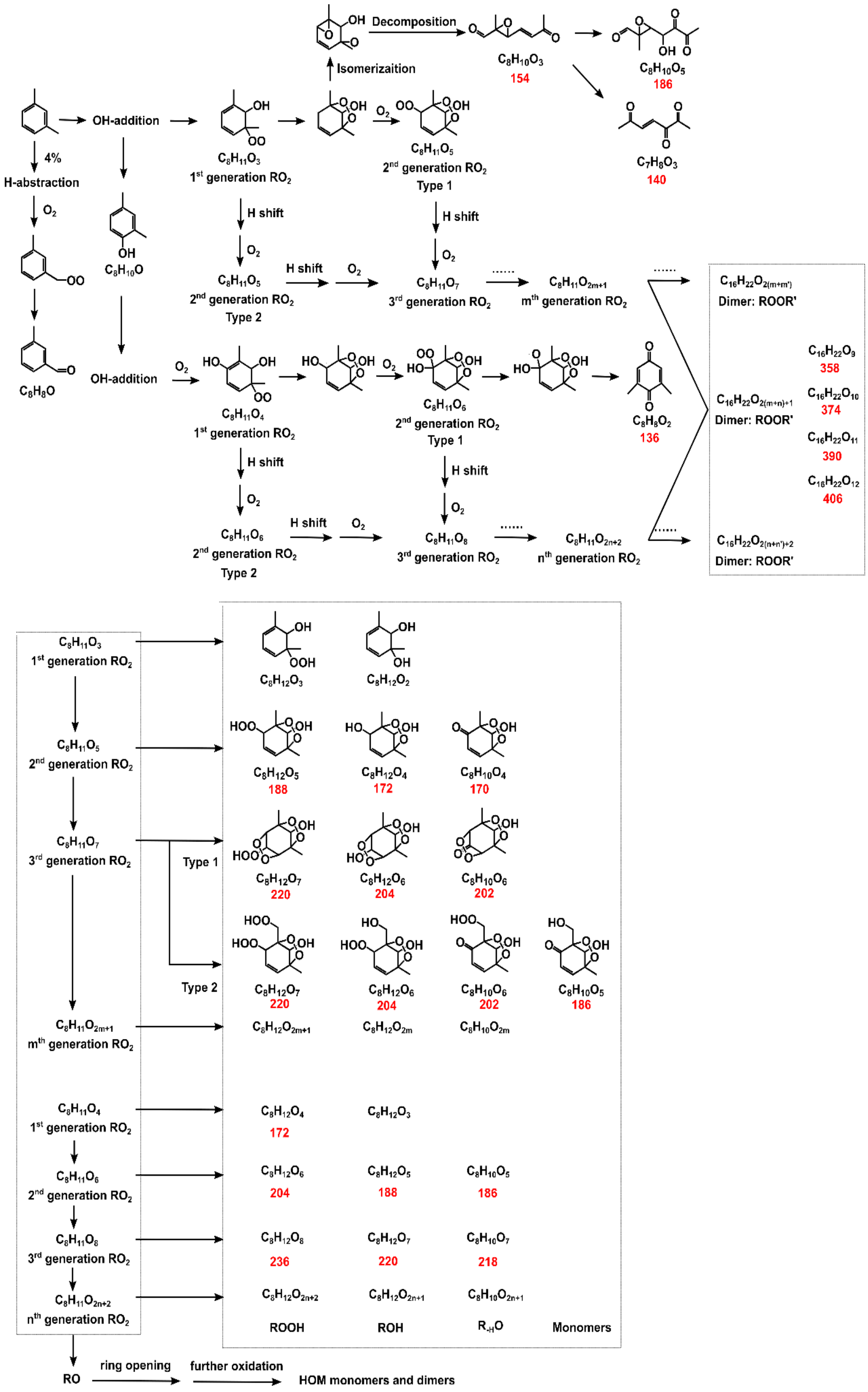

Scheme 1. The route of OH-initiated *m*-xylene oxidation. The red number below the molecular formula is its molecular weight, which is determined by HRMS to exist in the particle phase.

Table 1. Experimental conditions, SOA concentrations and yields at the end of the experiments in *m*-xylene-OH oxidation system.

Exp. No.	[*m*-xylene]$_0$ (μg m^{-3})	[*m*-xylene]$_{reacted}$ (μg m^{-3})	RH (%)	T (°C)	[SOA]$_e$ (μg m^{-3})	SOA yield (%)
1	2287.9	1026.3	13.6	25.9	150.3 ± 15.0	14.6 ± 1.5
2	1855.5	682.0	13.7	25.3	95.5 ± 9.5	14.0 ±1.4
3	2410.8	941.4	73.6	27.5	21.0 ± 2.1	2.2 ± 0.2
4	2029.1	946.9	79.1	27.4	7.5 ± 0.7	0.8 ± 0.1

[SOA]$_e$ indicates the mass concentration of SOA at the end of each experiment with particle wall loss corrected.

Table 2. Absorbance positions of functional groups and the intensities at low and high RHs.

Absorption frequencies	Functionality	Intensity (× 10^{-3})		Ratio [a]
		low RH	high RH	
3235	O-H	5.9	1.9	0.32
3000	C-H	4.5	1.4	0.31
1720	C=O	5.1	1.5	0.29
1415	CO-H	4.8	2.4	0.50
1180	C-O-C, C-O and OH of COOH	2.9	1.4	0.48
1080	C-C-OH	5.3	1.8	0.34

5 [a] Ratio of the intensity at high RH to that at low RH.

Table 3. Plausibility of different types of compounds with elemental formulae measured by HRMS in the positive ion mode.

Low RH			High RH				
Measured (m/z)	Intensity	Error (mDa)	Measured (m/z)	Intensity	Error (mDa)	Ion formula	Proposed structure
137.0596	1.7×10^6	0.6	137.0593	1.4×10^5	1	$[C_8H_9O_2]^+$	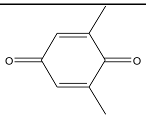
141.0545	5.6×10^6	1.3	141.0542	-	1.5	$[C_7H_9O_3]^+$	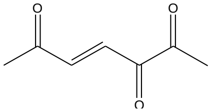
155.0701	1.0×10^6	1.2	155.0699	-	1.5	$[C_8H_{11}O_3]^+$	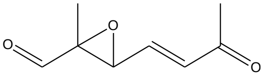
171.0651	1.0×10^6	1.2	171.0649	-	1.4	$[C_8H_{11}O_4]^+$	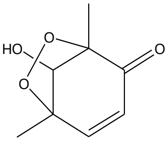
187.06	1.1×10^6	1.2	187.0568	-	4.4	$[C_8H_{11}O_5]^+$